Real-Time Stability Surveillance in Power Systems: A Deep Learning Approach

by Bhavesh Tukaram Shinde

B.S. in Electrical Engineering, June 2017, University of Mumbai

A Thesis submitted to

The Faculty of
The School of Engineering and Applied Science
of The George Washington University
in partial satisfaction of the requirements
for the degree of Master of Science

January 10, 2020

Thesis directed by

Payman Dehghanian
Assistant Professor of Electrical and Computer Engineering

Dedication

This study is wholeheartedly dedicated to the memory of my father the late Tukaram Shinde and my mother Rajubai Shinde who inculcated the importance of education in our family and supported me throughout the process of achieving my dreams.

I also dedicate this thesis to my brother, Ganesh Shinde and my sister, Komal Panchal who inspired me to attain my goals and for their constant motivation and encouragement through difficult phases of my life.

Without their sacrifice and unconditional love, my achievements would never be accomplished. It was all made possible because of their belief in me even after I continually failed to stand up to their expectations.

Above all, I dedicate my thesis to the GOD for His blessings throughout the completion of this thesis.

Acknowledgments

I would like to express my sincere gratitude to my advisor, Dr. Payman Dehghanian, for his guide, understanding, wisdom, patience, encouragements, and for supporting me reach this point. Thanks also to my committee members, Dr. Shahrokh Ahmadi and Dr. Milos Doroslovacki, for their time and patience.

Appreciation goes to my friends and the member of the Smart Grid Laboratory, namely Shiyuan Wang, Mohannad Alhazmi, Mostafa Nazemi, Zijiang Yang, Yifu Li, Dingwei Wang, Jinshun Su for making my time at the George Washington University a wonderful experience.

Most of all, I am fully indebted to my parents for their terrific support, without which, the pursuit of this advanced degree would never have been started and accomplished.

Abstract

Real-Time Stability Surveillance in Power Systems: A Deep Learning Approach

Online Power System Stability assessment is a critical problem which has enormous scope of development. Most electrical utilities investigate system stability by simulating critical contingencies to determine the severity of transient disturbances in the system. Assessment of power system transient stability is critical for a reliable and continuous operation and to ensure none of the working generating units in the system go out of synchronism. The main objective of this research is to develop a fast and robust online transient stability assessment tool to classify the system operating states and to identify system critical generators in case of instability. This research proposes a deep learning neural network framework that captures the phasor measurement unit (PMU) measurements and monitor the system transient stability in real-time. The proposed framework in a first case study utilizes the convolutional neural network (CNN) with hypotheses CNN pooling (HCP) to identify the system operating states and detect the set of critical generators. The proposed framework in the second case utilizes a hybrid deep learning network consisting of CNN and Long Short Term Memory (LSTM) called ConvLSTM network for the given problem of system stability monitoring. The suggested CNN-HCP module and ConvLSTM module for stability assessment and for detecting critical generators through multi-class and multi-label classifications are tested on the IEEE 118-bus test system and IEEE 39-bus test system, respectively, where different types of faults at different locations and under varying system load conditions are simulated. The test results verified that our proposed framework is fast and accurate, thereby a viable approach for online system stability monitoring applications.

Index Terms-Transient Stability Analysis, Convolutional Neural Network (CNN), Hypotheses CNN Pooling (HCP), Convolutional Long Short Term Memory (ConvLSTM) Network, Phasor Measurement Unit (PMU), Deep Learning.

Table of Contents

List of Figures

List of Tables

Nomenclature

0.1 *Abbreviations*

WSCC	Western System Coordinating Council
HVDC	High voltage direct current
PMU	Phasor measurement unit
CNN	Convolutional neural network
HCP	Hypotheses CNN pooling
LSTM	Long-short term memory
ConvLSTM	Convolutional long-short term memory
EAC	Equal area criterion
TDS	Time-domain simulations
TSA	Transient stability analysis
CCT	Critical fault clearing time
TEF	Transient energy function
PEF	Partial energy function
SMIB	Single machine infinite bus system
EEAC	Extended equal area criterion
SVM	Support vector machine
FCT	Fault clearing time
PE	Potential energy
KE	Kinetic energy
TSI	Transient stability index
FC-LSTM	Fully connected long-short term memory

0.2 *General Symbols*

V	Voltage magnitude
θ_v	Voltage phase angle
F	Frequency
I	Current magnitude
ω	Rotor Speed
$\Delta\omega$	Change in Rotor Speed
H	Per unit Inertia constant
$W_{kinetic}$	Kinetic energy
$S_B^{3\phi}$	3-phase apparent power
k	Damping constant
A_a	Accelerating area in power-angle characteristics graph
A_d	Decelerating area in power-angle characteristics graph
ω_0	Base electrical frequency
η	Transient stability index

0.2.1 *Angle Quantities*

δ	Measure of rotor Angle
δ_{max}	Measure of maximum rotor angle
δ^c	Measure of clearing angle
δ^0	Measure of angle before fault occurrence
δ^s	Measure of angle at post-fault stable condition
δ^m	Measure of peak angle during fault condition
$\Delta\delta$	Change in rotor angle

0.2.2 *Power Quantities*

P_M	Mechanical power
P_E	Electrical power
P_e^f	Electrical power during fault
P_e^p	Electrical power after fault

0.2.3 *Torque Quantities*

T_a	Accelerating torque
T_e	Electrical torque
T_S	Synchronizing torque
T_D	Damping torque
ΔT_e	Change in electrical torque

0.2.4 *Impedance Quantities*

L_d	Stator inductance for winding d
L_q	Stator inductance for winding q
M_D	Mutual inductance for stator to field damper winding
M_F	Mutual inductance for stator to q-axis damper winding
M_Q	Mutual inductance for stator to d-axis damper winding

0.2.5 *Time Quantities*

t_0	Initial fault clearing time
t_1	Lower time limit for a stable system

t_2	Higher time limit for a stable system
t_{mid}	Mean value of all time-limits

0.2.6 *Current Quantities*

i_d	Current magnitude in damper winding d
i_q	Current magnitude in damper winding q
i_D	Current magnitude in damper winding D
i_F	Current magnitude in damper winding F
i_Q	Current magnitude in damper winding Q

0.3 *Neural Network Symbols*

0.3.1 *CNN-HCP Network*

O_c^j	j^{th} feature map of convolutional layer
x_i	input image set
k_{ij}	convolutional kernel
b_j	bias in CNN network
W	weight in CNN network
β_j	j^{th} multiplier of pooling layer in CNN network
v_i	output vector of i^{th} hypotheses
v_{ij}	i_{th} component of output vector v_i
y_i	label vector for i^{th} image
$\hat{p}_i$	probability vector for i^{th} image
M	number of images
m_t	first order moment of gradient

v_t	second order moment of gradient
θ_t^i	i^{th} parameter value at time t
m_t^i	i^{th} component of vector m_t
v_t^i	i^{th} component of vector v_t

0.3.2 *ConvLSTM Network*

c_t	memory cell
i_t	input gate of the cell
o_t	output gate of the cell
f_t	forget gate of the cell
h_t	final state of the cell
b_i	bias corresponding to input gate equation
b_f	bias corresponding to output gate equation
b_o	bias corresponding to forget gate equation
Y	ground truth of ConvLSTM
$\tilde{Y}$	prediction value of ConvLSTM
L_{loss}	loss function of of ConvLSTM
P	probability distribution of of classification layer

Chapter 1: Introduction

There has been a rapid growth in the electric power systems since the evolution of interconnected power systems in 1940. Interconnected power systems render many advantages over the independent power systems as it represents an efficient but complicated generation, distribution and utilization of energy. Stability is a major issue in an extensively interconnected system as the disturbances in the system propagate quickly in the entire region, thus risking the integrity of the whole system. Loss of stability in the system can increase the possibility of cascade tripping i.e., a large part of the system will be damaged and other systems will be infected as well. Consequently, this can result in the system experiencing a number of blackouts due to dynamic instability conditions during credible contingencies [1]. Many areas of United States have experienced major blackouts or power outages over the years caused by power system instability problems. United States history comprises of 9 worst power outages from 1965 to 2012 which covered the West, East and Texas power grids and it affected over 140 million customers in all. The most severe amongst them were the 1996 failure in the Western System Coordinating Council (WSCC) interconnection system and the 2003 US-Canadian blackout which affected 50 million people from eight states in the US and two Canadian provinces. Therefore, the need for reliable and resilient operation of the power grid over the long run is much greater than ever before [6] [7].

Reliability of a power system signifies the ability to supply sufficient electric energy on continuous basis with fewer interruptions over an extended period of time. The term "reliability" in a power system refers to two components viz. security and adequacy [8]. Security of a power system is accomplished with the ability of the power system to endure unexpected disturbances such as electrical short circuits or unanticipated failures of system elements, without interruption of the electric service to the consumers at satisfactory frequency and voltages. Adequacy can be referred to the ability of the power system to

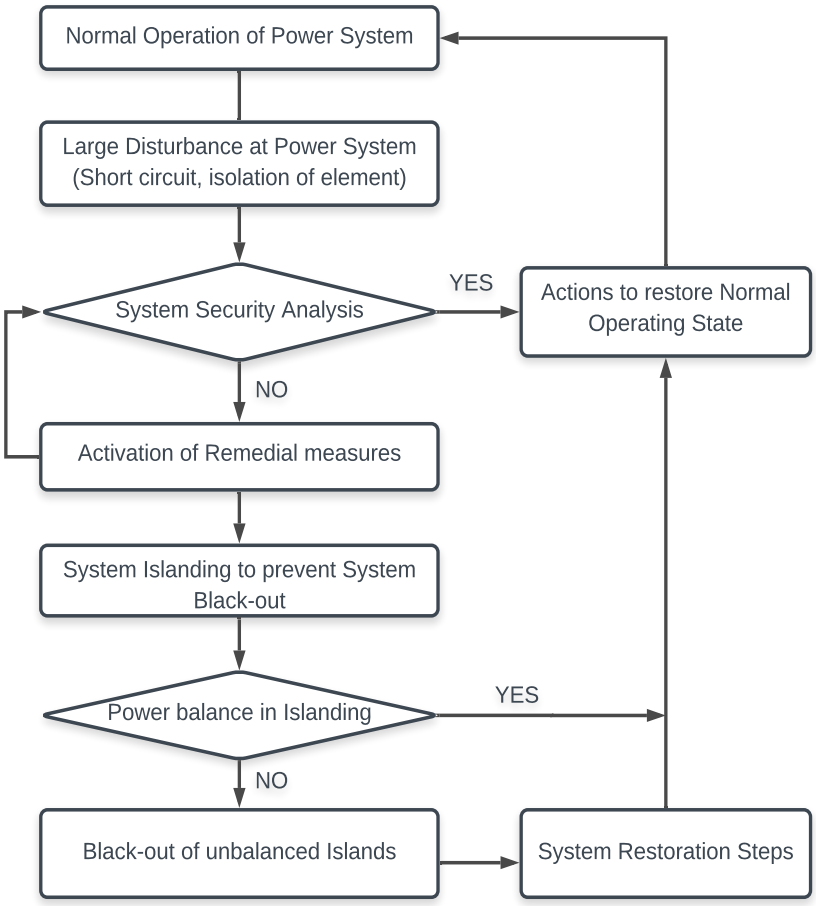

Figure 1.1: Operation State flow-chart for System Security [1]

supply aggregate electrical demand and energy needs at all times, taking into account the anticipated and reasonably expected unplanned failure of the system elements. Typically, power system reliability (and resilience) enhancement can be achieved through reliability (and resilience) enhancement techniques, health monitoring, and maintenance planning and scheduling of the grid components over time. While there are many efforts in the literature (including many of those published and presented at the GW Smart Grid Laboratory) in different domains (electric generation, transmission, and distribution) on enhancing the network and component reliability, cost-efficiency, and resilience through advanced smart grid technologies [9–78], such improvements in the component and infrastructure may be a medium-term and long-term effort (e.g., preventive maintenance plans) which may not be accomplished in a short time frame [9, 79–99]. Reliable operation of the grid requires

advanced tools for online power system stability surveillance that can process massive data corresponding to a wide range of network connectivity and generation dispatches during normal and abnormal conditions. Figure 1.1 depicts a flow-chart of the power grid operating states by continuous evaluation of system states to assure secure and reliable operation of the grid along with the necessary actions needed to be taken during abnormal conditions.

1.1 On the Concept of Power System Stability

Power system stability has been recognized as an important problem for secure system operation since the 1920's [100, 101]. The importance of power system instability has been brought into notice by the occurrence of many major blackouts in the system [102]. In a power system, the synchronous machines are continuously operating in synchronism. A stable power system condition requires that these synchronous machines must maintain synchronism under all steady-state conditions. During a disturbance in the system, the system establishes a force in order to normalize or stabilize the system operating state.

Definition: *"Power system stability is the ability of an electric power system for a given initial operating condition, to regain a state of operating equilibrium after being subjected to a physical disturbance, with most system variables bounded so that practically the entire system remains intact."* [2]. The definition applies to an interconnected power system as a whole. The system integrity is maintained when practically the entire power system remains intact without the tripping of generators or loads, except for those disconnected by isolation of the faulty components and purposely tripped to ensure the operational continuity of the rest of the system. Stability is a condition of equilibrium between opposing forces [2];instability is a result of a sustained imbalance between these opposing forces in case of a disturbance. The power system is a highly non-linear system that operates in a constantly changing environment; loads, generator outputs, topology and key operating parameters change continually. A remote generator or any particular loads or load areas may lose stability (out of synchronism for generators, running down in case of loads) without

cascading instability of the main system. The stability of the system depends on the nature of the disturbance and also, on the initial operating condition when exposed to a transient disturbance. The high dimensionality and complexity of the stability problems has drawn attention towards importance of simplifying assumptions and evaluation of different types of problems using the right degree of detail for system representation.

A wide range of disturbances both small and large disturbances are observed in a power system [47–50, 52–54]. Small disturbances include load changes that occur continually and the severe one's include short circuit on a transmission line or loss of large generator. A power system must be capable enough to withstand small disturbances occurring at different times in the system; adapt itself to the changing conditions and operate in a satisfactory manner [47–49]. At times, it is even expected to survive numerous sever disturbances except for the conditions where the disturbance may result in structural changes due to isolation of faulty elements. If the power system is stable after a transient disturbance, it will gain a new equilibrium state with practically the entire system intact; the actions of automatic controls and possibly human operators will eventually restore the system to a normal operating state [103]. On contrary, if the system becomes unstable, it will result in a run-down condition, such as a progressive increase in separation of rotor angles or a progressive increase in bus voltage magnitudes. For a particular physical disturbance, a power system may be stable at an equilibrium set, or unstable otherwise. It is practically and economically impossible to design a power system to be robust for every possible disturbance. The selection of design contingencies are done based on the consideration that they have a high probability of occurrence. Therefore, stability of a large disturbance always refers to a specified disturbance condition. A stable equilibrium set has a finite region of equilibrium, i.e., the larger the region, the more robust the system with respect to large disturbances [2].

A disturbance in power systems may lead to a response which involves many equipment such as, a fault on a critical element followed by its isolation from the system will cause ad-

verse effects in the system. The protective devices used to protect individual equipment may counter the variations in the system variables and, thereby, affect the system performance factor. Due to the modern power system being a very high-order multi-variable process influenced by a wide array of devices with different response characteristics, instability in a power system may occur in various different ways depending on several factors such as type of the disturbance, system operating state when disrupted and its topology. Traditionally, stability has been directly linked with the maintenance of synchronous operation, since power systems rely on synchronous generators for the generation of electrical power. The dynamics of generator rotor angles and power angle relationships is the major influence over this aspect of stability. Several other factors other than loss of synchronism of the generator machines can lead to instability conditions in power systems. For instance, instability in load voltage or in the system frequency may occur, ultimately lead to black-out in few cases. Since power systems undergo continuous fluctuations of small magnitudes, stability assessment during the instance of specified disturbances becomes important and it is valid to consider that the system is initially in a true steady-state operating condition [2].

1.2 Power System Stability Classification

On a broader view, power system stability is considered to be a single problem; however, various types of instability problems that may occur in a power system is difficult to be understood and dealt with. Stability analysis which includes identification of key factors contributing to instability and the development of methods to improve stable operation, is greatly facilitated by classification of stability into appropriate categories [104]. This illustrates importance of classification of power system stability problems for meaningful practical analysis of the system. Classification is justified theoretically by the concept of partial stability of a power system [105] [106]. The classification of power system stability proposed in [104] is based on the following considerations:

- The physical nature of the resulting mode of instability as indicated by the main

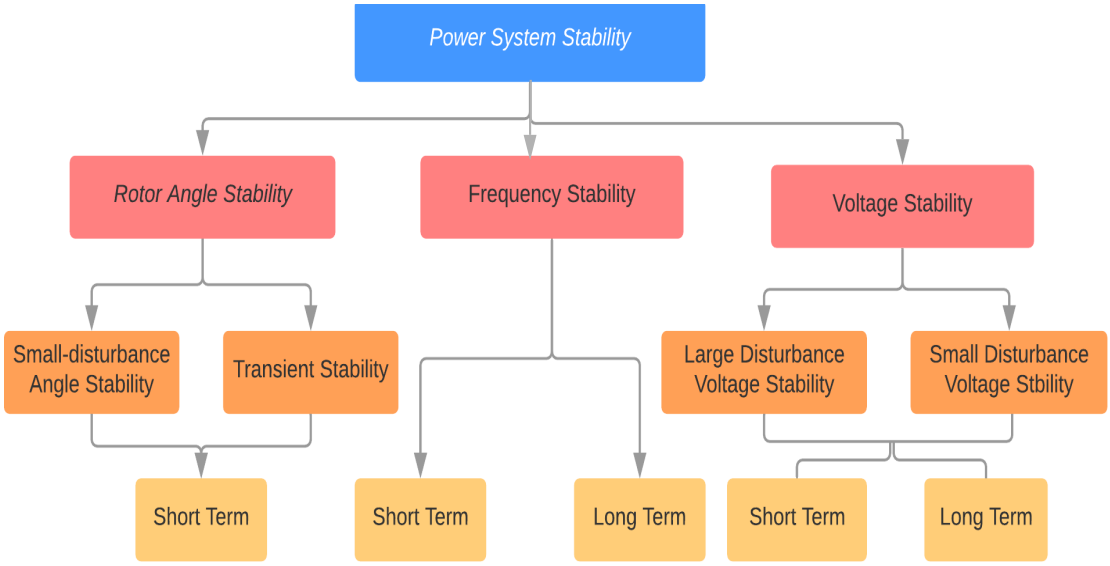

Figure 1.2: Classification of Power System Stability [2]

system variable in which instability can be observed.

- The size of the disturbance considered, which influences the method of calculation and prediction of stability.

- The devices, processes and the time span to be considered to assess the system stability conditions.

Figure 1.2 shows the overall classification of power system stability, identifying its categories and sub-categories. *Short-term* voltage stability includes dynamics of fast acting load components such as HVDC converters, induction motors and electronically controlled loads. *Long-term* stability is associated with disturbances present for longer durations which causes adverse effects on large-scale systems resulting in inconsistency between generation and consumption of power. The long-term and mid-term stability are comparatively recent additions to the literature on power system stability. In *mid-term* stability, the focus is on synchronizing power oscillations between machines, including the effects of some of the slower phenomena and possibly large voltage or frequency excursions [104].

Rotor Angle Stability: There are possibly three different forms of instability conditions in a power system: rotor angle instability, voltage instability and frequency instability. The ability of the interconnected synchronous generator machines in a power system to remain in synchronism is known as *Rotor Angle Stability*. As seen from the Figure 1.2, rotor angle stability has two main sub-classes: small disturbance (steady-state) stability and large disturbance (transient state) stability. Small disturbance stability is directly dependent on initial operating state of the system. The reason of instability in this case may be due to (i) the increase in rotor angle because of lack of synchronizing torque, or (ii) increase in rotor oscillations amplitude because of insufficient damping of oscillations. Small disturbance stability problems can be global or local in nature. Global problems are caused by interactions between large groups of generators and they have widespread effects on the power system. Whereas, local problems are associated with local plant mode oscillations of a single power plant and it involves a small part of the power system. The time-frame consideration of small disturbance stability studies is normally around 10 to 20 seconds following a disturbance. On the other hand, large disturbance stability, also called as transient stability, is dependent on both the initial operating condition of the system and severity of the disturbance in the system. Instability is caused mainly due to insufficient synchronizing torque resulting in aperiodic angular separation, demonstrating first swing instability; however, a local plant swing mode or a slow inter-area swing mode may cause a wide rotor angle excursion beyond the first swing. The time-frame consideration in case of transient stability studies is typically 3 to 5 seconds but may extend to 10 to 20 seconds following the disturbance for large systems. Stead state stability as well as transient stability are further categorized as short term phenomenon.

Voltage Stability: *Voltage Stability* refers to the ability of a power system to maintain acceptable voltages at all buses under normal operating condition and on undergoing a disturbance. Voltage stability is related to maintenance and restoration of equilibrium between demanded load and supply from the power system. The possible adverse effects

due to voltage instability are loss of loads, tripping of transmission lines or other elements, cascading outages and these may further result in loss of synchronism of generators. The main reason for voltage instability is voltage drop occurring due to the flow of active and reactive power through inductive reactances of the network. Although voltage drop being the common contributing factor to this instability condition, the risk of overvoltage instability also exists. The problem of uncontrolled overvoltages is due to the self-excitation of synchronous machines which arises when the capacitive load of the machines is immensely large. Similar to the classification of rotor angle stability, voltage stability is also classified into two sub-categories: large disturbance voltage stability and small disturbance voltage stability. The ability of the voltage stability is determined by the system and load characteristics and the interactions of both discreet and continuous controls. Monitoring of the non-linear response of the power system over a period of specified time to track the interactions and performances of devices helps to determine large disturbance voltage stability. The time-frame consideration for large disturbance voltage stability may extend from few seconds to tens of minutes. Small disturbance voltage stability is influenced by continuous controls and discrete controls at any given time and characteristics of loads. This concept is utilized to determine the behaviour of the system voltages in response to small system changes at any given instant. A combination of linear and non-linear analysis of system equations in a complementary manner is typically utilized to identify the stability influencing factors. The time-frame consideration of small disturbance voltage stability is similar to the prior one and therefore, voltage stability in general can be either short-term or long-term. The distinction of voltage stability with rotor angle stability is on the basis of specific set of opposing forces experiencing a sustained imbalance and the system variable in which the resulting instability is evident.

Frequency Stability: When being subjected to a severe disturbance in the power system leading to imbalance between generation and load, its ability to maintain steady frequency is known as *Frequency Stability*. Frequency stability is related to maintenance and restoration

of equilibrium between system generation and load with minimum loss of load. Sustained frequency swings which could possibly result in tripping of generating units or loads are the main causes of this instability condition. Frequency instability is associated with problems such as poor coordination of control and protective elements, inadequate responses of equipment or dearth of generation reserve [107]. As identified in 1.2, frequency stability can be classified as short-term or long-term phenomenon. Short-term frequency instability is the formation of an undergenerated island with insufficient underfrequency load shedding such that frequency decays rapidly causing blackout of the island within a few seconds [107]. Frequency instability caused because of more complex situations such as speed turbine or reactor control and protection are long-term phenomena [108].

Amongst these different categories of power system stability, this research will focus on the first category, i.e., the rotor angle stability in general and the transient stability in particular. In short, the stability study involving large disturbances due to imbalance between mechanical input and electrical output powers. The focus being on first swing periodic drift, the transients can be observed in fraction of a second and several simulation time-steps to study the system. It occurs when the system lacks synchronizing torque or when an unstable control action is taken [109].

1.3 On the Concept of Transient Stability Analysis

Transient stability is the ability of a power system to withstand a sudden change in generation, load, or system characteristics without a prolonged loss of synchronism [110]. A transient disturbance in the network or generator may cause some oscillations as the mechanical torque is incapable of balancing out the transient variation in electric torque. Electrical power output of a synchronous machine can be resolved into product of electrical torque and speed. Further, after a transient disturbance in the system, the change in electrical torque

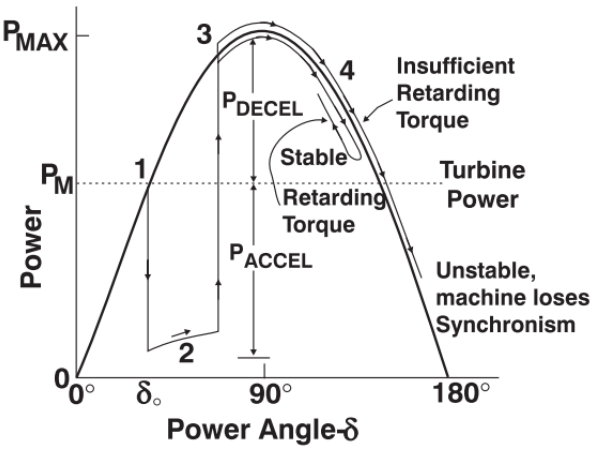

Figure 1.3: Demonstration of the Power Grid Transient Stability [3]

can be resolved into two components:

$$\Delta T_e = T_S \Delta\delta + T_D \Delta\omega \tag{1.1}$$

$T_s\Delta\delta$ is the component of torque that is in phase with the rotor angle change. This is know as the "synchronizing torque". $T_D\Delta\omega$ is the component of torque that is in phase with the speed change. This is known as the "damping torque" [3].

Both of these torque components act on each generator in the system. Loss of synchronism is the result of insufficient synchronizing torque which can be prevented if enough magnetic flux can be produced when there is occurrence of a transient change in the electrical torque. When the rotor accelerates in relation to the stator flux, the rotor angle increases due to mechanical torque being higher than the electrical torque. In this case, high positive voltage to the alternator field by the exciter system can increase the excitation. Conversely, during the cases of decreasing rotor angle, application of high negative voltage to the alternator field to decrease the excitation is necessary.

The major concerns related to transient stability are observed following the effects of the generator asynchronism or transmission line disturbances. Figure 1.3 shows the behaviour of a generator post-fault condition. A transmission fault in the system causes the generator

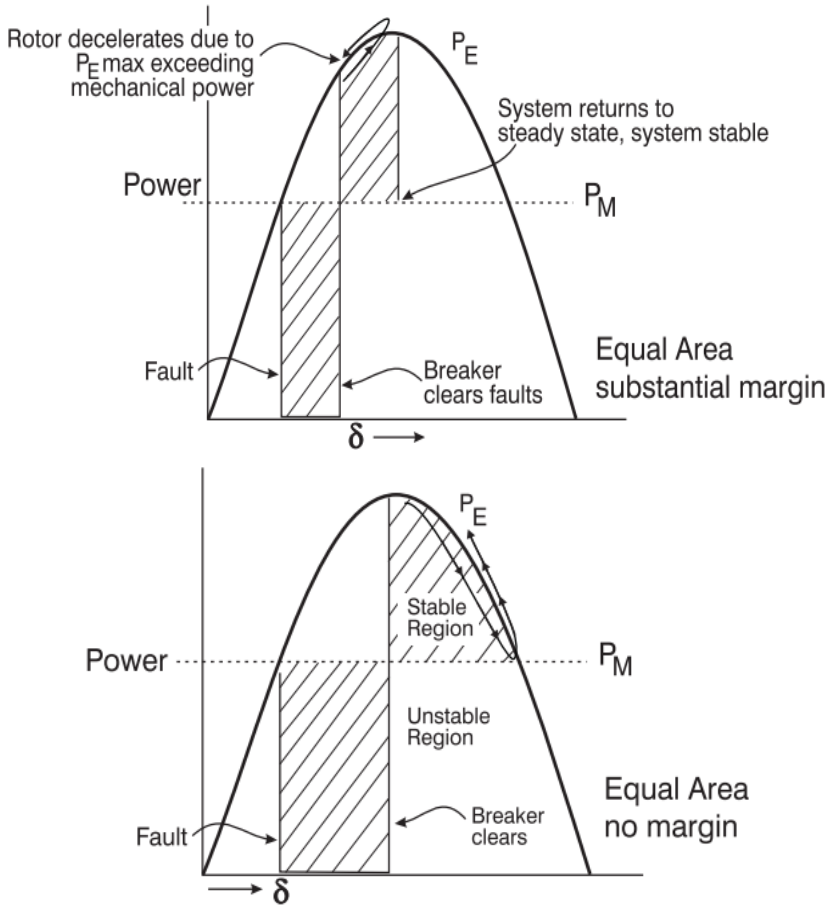

Figure 1.4: Effect of Fault Clearing Time on Power Grid Transient Stability [3]

electrical output power to be reduced to a greater extent (at point 1). The difference between the electrical power and the mechanical power causes an increase in the power angle (at point 2). Post-fault clearance, the electrical power is restored to an appropriate level which corresponds to a point on the power angle curve (at point 3). When the fault is cleared, one or more transmission elements are removed from the system, thereby increasing the electrical power of the generator above the turbine power. This will lead the generating unit to decelerate (at point 4). The generator synchronism with the power system depends on the retarding torque whether it is sufficient or insufficient to make up for the acceleration during the fault.

For a fault on the transmission line, power system stability depends on the clearing time of the fault [3]. As shown in Figure 1.4, when the fault clearing process is slow, the

extended period of fault allows the rotor to accelerate further along the curve of electrical power output. whereas, faster fault clearing time prevents the acceleration of rotor much sooner, assuring the system is recovered with sufficient amount of synchronizing torque. For transient stability analysis, the system needs to be analyzed using the non-linear swing equation that describes the rotor acceleration/deceleration with regards to the load changes or current flow in the stator circuit [111–113].

1.4 Problem Statement

Transient Stability Assessment is the most critical to perform and monitor in power systems. Various industry-grade transient stability simulation tools give considerably different results for similar power system models [114]. In a running system, many small anticipated and unanticipated changes are occurring which underlines the need for an adaptive and intelligent method to determine the transient instability in the system. Transient stability assessment, as a mechanism to capture the power system dynamic security conditions, plays a significant role in day-to-day power system operation. This is particularly critical due to the following: (i) continuing growth in the system interconnection size and complexity; (ii) proliferation of renewables and rushing arrival of uncertainties; (iii) the increasing demand for electricity. As the power system operating point is reaching the stability limit and its control becomes more challenging and difficult, the instability problem is more likely to occur [115], which would potentially lead to system outages and blackouts [116]. Therefore, the online monitoring of electric power system becomes more and more important in order to evaluate and enhance the performance of the system operation at different loading levels due to extensive number of system contingencies. The main responsibility of the independent system operator is to manage power system security at all operating conditions well ahead of time. There is an increased risk of generator machine losing synchronism during abnormal conditions occurring due to system instability. Thus, along with accurate online monitoring of the system to determine its operating state, the behaviour of all the generators connected in the

system must be monitored to keep the generators in synchronism.

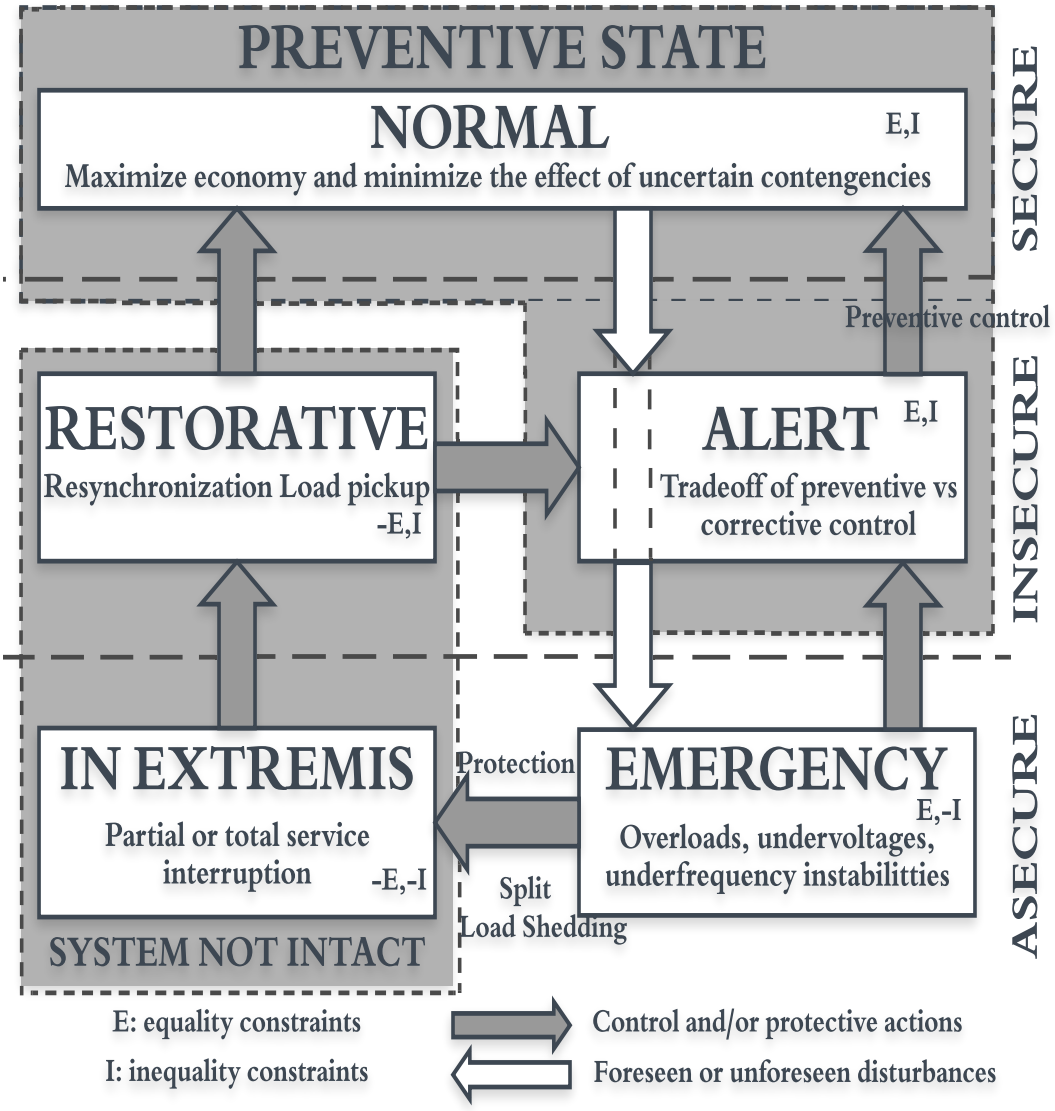

Figure 1.5: Power System Operating States

It is important to know the operating states that a power system may experience in real-time operation which are explained as follows:

- **Normal State:** In this state, the system parameters such as voltage, frequency, current etc. are within the normal and desired range of operation.
- **Alert State:** In this state, all system parameters are within an acceptable range but very close to their limits.

- **Emergency State:** In this state, some system parameters are outside their acceptable range and some loads may lose power. This may lead to system disintegration.

- **Extremis State:** In this state, partial or system wide black-out may occur.

- **Restorative State:** In this state, the system goes into a process of restoration by reconnecting system elements and re-synchronizing generators to achieve the normal operating state.

Figure 1.5 shows the "Dy-Liacco diagram" which displays detailed description of different operating modes in a power system [117].

The classical analysis of power system stability requires a complete system modeling and is time consuming for large power systems in addition to the dependence of the dynamic behavior on the load conditions and the severity of critical contingencies on the system operations [1]. Therefore, development of real-time computational tools for online monitoring of power system transient stability is the main target of this research thesis. The post-fault contingencies need necessary measures to release the effects of the fault on the system, thus the system operator needs fast and accurate online monitoring tools to activate the correct control measures during an abnormal operating condition. Due to the uncertainty associated with large scale power system operation, it is important to detect the critical generator machines well ahead of time to reduce the effects of large disturbances on the system stability and ensure a stable operation of the power system at all times.

In the proposed framework for online power system stability surveillance, firstly, the system variables (voltage, current, voltage angle) data is obtained from the phasor measurement units (PMU) installed at all generator buses. In addition to the PMU system parameters, rate of change of angle i.e. frequency is used as the fourth variable. Also, rotor angle and rotor speed of the machine are used as two different variables along with the four variables mentioned above. Although rotor angle and rotor speed measurements are not directly available from PMU measurements, they can be estimated using various dynamic state estimation

methods [118–123] . Hence, for the proposed online power system stability monitoring model, these six variables are used as the input data. The proposed framework for power system surveillance is divided into three parts viz. collection of data from PMUs, offline training of the deep learning neural network model and online application in real-time to monitor the power system stability. This research study involves application of the proposed model on two different power system test cases using different deep learning models in each case. For the first case study, Convolutional Neural Network (CNN) with Hypotheses CNN Pooling (HCP) model is tested on the IEEE 118-bus test system and for the second case study, a hybrid model combining CNN and Long-short Term Memory (LSTM) model is applied and analyzed on the IEEE 39-bus test system.

1.5 Thesis Outline

Chapter 1 gives a detailed overview on the theoretical aspects of power system stability. Further, it introduces different types of stability problems occurring in power systems and describes transient stability analysis in detail. The chapter draws the attention to the main research problem resolved in this thesis.

Chapter 2 provides a historical background on the stability problems in power grids and summarizes a detailed description and formulation of the various approaches used to assess the transient stability over the period of the past century. Further, the thesis introduces two case studies with two novel approaches for the transient stability assessment. The main focus of the implementation of the proposed techniques is to improve the performance of the online transient stability assessment compared to the previously developed models. A reference on utilizing heat-map images to monitor the stability of the power system is being implemented in this thesis research.

In Chapter 3, the method of converting the system measurements from PMUs located at generator buses to the heat-map images is demonstrated. There is a use of data which are not directly available from PMUs but can be formulated using dynamic state equations; hence,

Chapter 3 explains the formulation derivation of such system variables such as rotor angle and rotor speed using damper current windings. The chapter presents the proposed CNN model with the use of HCP pooling for performance enhancement on detection of critical generators in case of instability conditions. The proposed deep learning neural network is displayed and described in detail with related mathematical equations. The process of data collection and processing of different types of faults at various loading levels in the IEEE 118-bus test system is explained. Further, the numerical results of the proposed model is analyzed and compared with previously proposed models.

In Chapter 4, a similar approach for tracking the stability of the power system in real-time using heat-map images is justified with improvements in addition accountable data and expansion of scope of training the deep learning model for more severe disturbances in order to build a highly robust and secure online monitoring assessment tool. The proposed deep learning network developed for this study is the hybrid Convolutional LSTM approach which is being implemented on the IEEE 39-bus test system to test its results and performances. Further addition of system variable to the already existing set of variables in a data matrix to enhance the reliability of the proposed model and inclusion of dual-order fault contingencies in the training data set are shown in this chapter. The numerical results of the proposed advanced ConvLSTM model are discussed and a conclusion is drawn based on the obtained results. Lastly, a conclusion based on the two different approaches used for transient stability assessment is done along with an explanation of the future research work that could be possibly achieved in this area of study.

Chapter 2: Literature Review

2.1 Background on Power System Stability Problems

Considering numerous types of power system instability problems that have emerged over the last century, various different methods such as stability theories, control technologies and computational tools were developed in response to the power system stability analysis problems. Review of the history of this topic to better understand the different methodologies used previously to tackle the stability problem is necessary in order to develop advanced strategies and modern solutions that can holistically address the challenges. The attention towards stability problem was drawn back to 1925 when problems associated with remote power plants feeding load centers over long transmission lines were encountered [109]. Steady-state and transient state instability often led to limitation of power transfer capability due to insufficient synchronizing torque as the exciters and voltage regulators were not the advanced ones that are seen today.

Initially for the early systems, graphical methods like Equal Area Criterion (EAC) and power circle diagrams were developed. With the growing system sizes and interconnected systems coming into picture, the system became more complex and thus leading to more complex stability problems. 1930 saw the development of network analyzer to analyze power flows in the grid and improve the stability calculations. Thereafter, development of electronic analog and digital computers after 1950 changed the face of power system stability analysis. After 1960s, large interconnected systems came into picture when the power systems in United States and Canada were joined as two major east and west systems. During early 1970s, large system breakdowns due to frequency instability led to the study of associated problems and development of dynamic simulation programs for their analysis. Most industry efforts were concentrated on transient stability problems leading to development of powerful simulation programs capable of modeling large complex power

systems. Due to advancements in all sectors of the society, there has been an increased stress on the grid operation which have resulted in numerous challenges for its secure operation. Increasing complexity in power systems and consideration of all forms of instability problems require careful planning and modeling of the power grid. In recent years, significant progress has been made to develop better tools and techniques for power system stability analysis.

2.2 Review of Transient Stability Analysis Methods

As stated in the previous section, the first method developed for stability analysis was the graphical methods such as EAC and the power circle diagrams. These methods were typically applied to the early systems which were represented as two-machine systems [124]. As the complexity and the system size grew, these methods were soon outdated as the problems became too complex to be dealt with these graphical methods. For multi-machine systems, the traditional methods through time-domain simulations (TDS) [125] which are efficient for critical fault clearing (CCT) time calculation is the mainstream Transient Stability Analysis (TSA) approach in power systems. However, it requires high computations for solving non-linear differential algebraic equations and it is not suitable for online applications due to its computational complexity. Application of Transient Energy Function (TEF) [126], which is used to determine CCT for TSA of multi-machine power systems was based on classical models. Using TEF, CCT could be determined accurately with comparatively less computational time than TDS or any other numerical methods, but it still suffers from modeling limitations which eventually affects simulation of large power systems. Partial energy function (PEF) [127] which compare the potential and kinetic energy values of the system against the reference values for calculation of CCT have presented drawbacks in accurately estimating the actual energy values in practical scenarios. Energy function methods and their variations are abundantly used with limited success in stability analysis of large-scale power systems. A method was proposed to decompose multi-machine system

into two subsystems, such that each subsystem is replaced by an equivalent machine to replicate it like a two-machine system [128]. Further, the two-machine system is reduced to a single machine infinite bus model (SMIB) [129]. For the reduced SMIB model, Extended Equal Area Criterion (EEAC) is used to calculate the CCT for transient stability analysis. EEAC and other trajectory convexity-concavity methods that assess the transient stability based on the SMIB model are computationally more efficient, but the performance accuracy is being compromised.

The latest methods proposed are based on the time-series models for time-adaptive transient stability assessment in power system. In recent years, many techniques based on data driven models and machine learning analytics have been explored to assess the system stability performance via online fault detection and classification [130–136]. There have been studies based on Support Vector Machine (SVM) machine learning methods [132, 137, 138] for assessing power system transient stability which were found successful. In comparison with various other machine learning models such as decision tree, regression, multi-layer perceptron or rule based methods mentioned above, SVM methods have shown far more effective and superior results for transient stability assessment. SVM is seen to produce better results while assessing transient stability; however, in certain situations, inaccurate information of post-fault conditions lead to significant degradation of the model performance. Long short-term memory (LSTM) [139] methods are effective while dealing with feature extraction in time dimension, but due to their disadvantages in parallelization, training stability and inference speed, feed forward models in time-series classification are preferred. Thus, the need for a more robust models which are independent of various drawbacks faced with different machine learning techniques is evident.

2.3 Formulation of Traditional Transient Stability Analysis Models

If a severe transient disturbance occurs in power systems, adverse effects such as loss of load, loss of generator or transmission system faults are encountered potentially leading to

loss of synchronism. In such cases, within two to three seconds following the occurrence of the disturbance, transient instability is evident. Before the introduction of formulations for some of the TSA methods, it is essential to understand swing equation to represent the dynamics of the system.

Swing Equation: The rotational dynamics of the synchronous generator machine is given by the swing equation which is used in stability analysis. When a disturbance is subjected into the machine, the fixed position of the rotor and resultant axis is disturbed due to acceleration or deceleration of the rotor [4]. The swing equation of a power system is given as:

$$M\ddot{\delta} + D\dot{\delta} + P_G(\delta) = P_M^0 \tag{2.1}$$

where $M \triangleq H/\pi\ f_0$

H is the per unit inertia constant,

$$H \triangleq \frac{W_{kinetic}^0}{S_B^{3\phi}} = \frac{kineticenergy}{3-phaseapparentpower} \tag{2.2}$$

$D \triangleq 2\ k\ \omega_0\ /\ S_B^{3\phi}$

$P_G(\delta)$ is the electrical power in p.u.

P_M^0 is the mechanical power in p.u.

δ is the relative angle of the electric power

k is the damping constant

ω_0 is the base electrical frequency in rad/sec

With an idea of the swing equation, the formulations of some of the traditional approaches of transient stability analysis are discussed below.

Equal Area Criterion: For a SMIB system, solving the swing equation is not required to determine the increase or decrease in the rotor angle values. Assume a purely reactive system with constant mechanical power P_m and constant voltage for transient reactance for the system. Assume a 3-phase fault appearing in the system and it is being cleared at t=0.

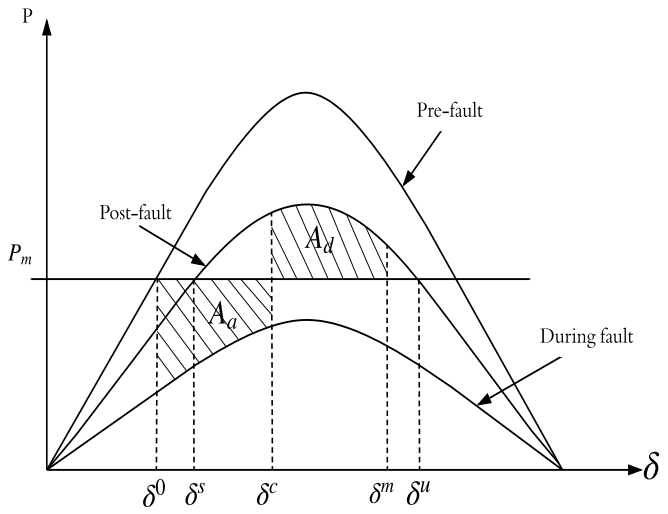

Figure 2.1: Power-Angle Characteristic of the Power System

The power-angle characteristics of the system when the line is opened to clear the fault are described in Figure 2.1. In the figure, δ^0 and δ^s are the pre-fault and post-fault stable equilibrium points of the system. When the fault takes place in the system, generator accelerates as the electrical power output almost goes to zero and the power angle δ increases and when the fault is cleared by removing the faulted line, the electrical power rises above the mechanical power, the generator decelerates and the angle δ decreases and reaches a minimum value from where it starts increasing again. The generator angle will settle down at δ^s after oscillating there for sometime because of system damping. The peak angle δ^m can be determined for a given clearing angle of δ^c by equating area A_a (accelerating area) to area A_d (decelerating area).

The expression for A_a and A_d are given as follows:

$$A_a = \int_{\delta^0}^{\delta^c} (P_m - P_e^f) d\delta \tag{2.3}$$

$$A_d = \int_{\delta^c}^{\delta^m} (P_e^p - P_m) d\delta \tag{2.4}$$

where, P_e^f is the electrical power during fault and P_e^p is the electrical power after fault.

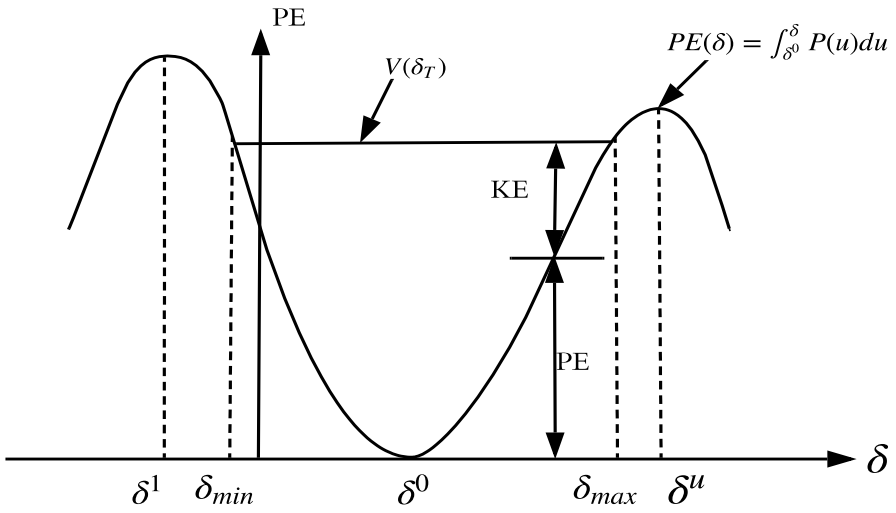

Figure 2.2: Potential Energy Curve [4]

In a transient stable system, maximum A_d is greater than A_a i.e ($A_d > A_a$). When A_d and A_a are equal ($A_d = A_a$), the maximum CCT is achieved.

Lyapunov's Method: According to M. Lyapunov, in a non-linear dynamic system of dimension n, the stability of the equilibrium is stated as:

$$\dot{x} = f(x), \quad f(0) = 0 \tag{2.5}$$

Lyapunov's theorem states that if there exists a scalar function $V(x)$ for Equation 2.5 that is positive-definite around the equilibrium point "0" and the derivative $\dot{V}(x) < 0$, then the equilibrium is asymptotically stable [140]. $\dot{V}(x) < 0$ can be obtained as:

$$\dot{V}(x) = \bigtriangledown V^T \cdot f(x) \tag{2.6}$$

$V(x)$ is a generalization of the concept of energy of the system. Lyapunov's sum of energy functions have provided the best results over other Lyapunov functions. In power world, Lyapunov's method has become the so called Transient Energy Function method [140].

Time Domain Simulation (TDS): TDS deals simultaneously with the system differential equations and algebraic equations to simulate the dynamic behavior of the power system

under fault conditions [1]. TSA is usually performed in system planning and the methods used for TSA analysis is time-domain numerical integration. TDS starts by solving load flow problem which gives pre-disturbance state data. The estimation of the system variables at the next time step can be performed using values of the current time step by integration techniques [141]. The swing curves that represent the rotor angle of each generating machine are compared with each other to determine if the rotor angle difference of any two machines exceed the limit of 360 degrees. The system becomes transiently unstable if the angular difference exceeds the predefined limit. Critical Fault Clearing Time (CCT) is the longest fault duration that prevents any generator to go out of synchronism in the system such that power system is transiently stable. CCT associated with any particular contingency depends on the configuration of the system and loading level during fault occurrence. In order to calculate CCT, TDS method is applied for all industrial system planning during contingencies. In many previous work based on stability monitoring, CCT has been used as an index to monitor the power system transient stability. CCT is utilized for TSA to identify stable and unstable cases and select the most severe contingencies.

Online or offline estimation of CCT is done to specify transient stability index, but the computation is time consuming. Bisection technique to evaluate CCT using TDS helps to reduce the computation time to some extent [142]. The flow chart of the Bisection technique is illustrated in Figure 2.3 [1]. The technique starts from initial fault clearing time (FCT) and if the CCT is found within the time boundaries ($t_0 \pm \sigma$), the CCT can be estimated using Bisection technique. For the stable system, lower limit (t_1) is replaced by the mean value (t_{mid}), otherwise, higher limit (t_2) is replaced by the mean value (t_{mid}) during the next step calculation. The CCT is selected as higher limit when the acceptance tolerance, ε, between the limits is satisfied. Upon estimation of CCTs, the set of contingencies are ranked and the contingency with the lowest CCT value is categorized as the most severe contingency. The time required to classify the system operating states based on calculation of credible contingencies is still high to be implemented in online applications.

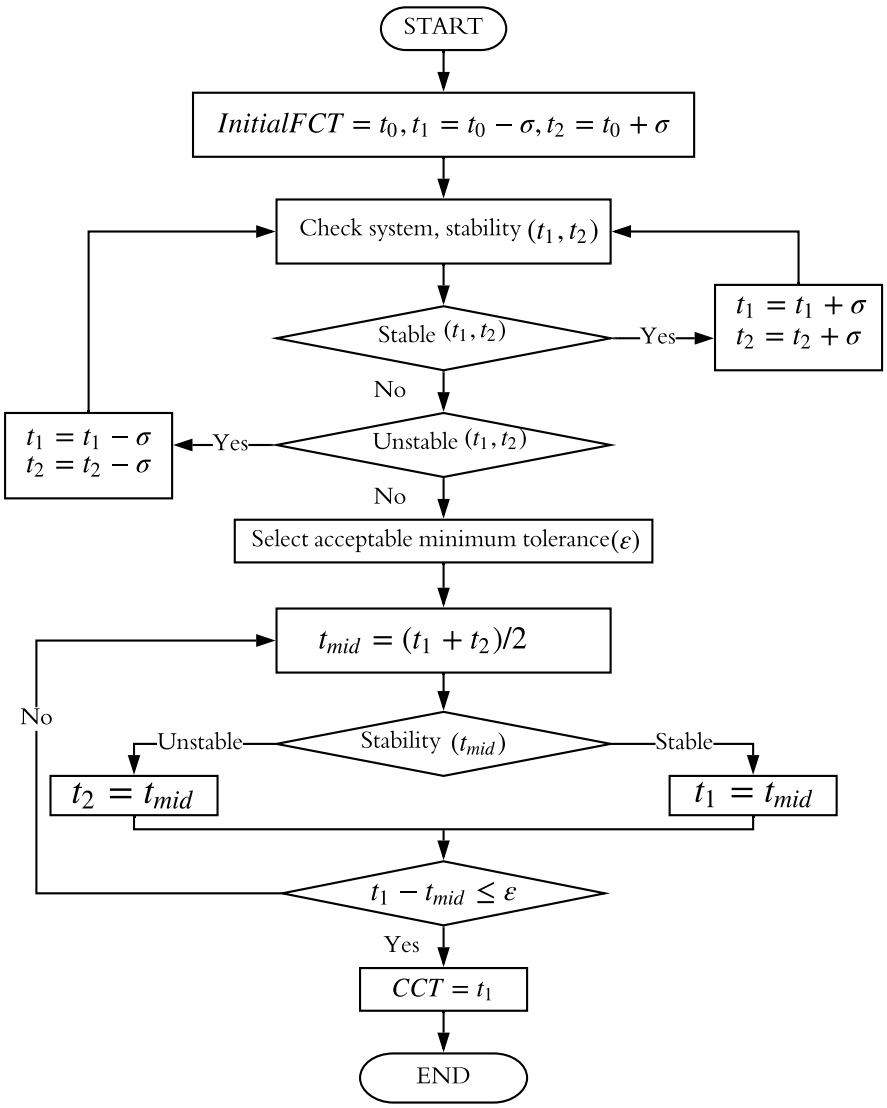

Figure 2.3: CCT Estimation using Bisection Technique

Transient Energy Function (TEF): Since the potential energy (PE) and kinetic energy (KE) are constant, the total energy of the system in terms of δ can be stated as:

$$V(\delta) = \frac{M\dot{\delta}^2}{2} + \int_{\delta^0}^{\delta} P(u)du \tag{2.7}$$

At equilibrium point, both PE and KE are zero, and hence, the after the fault clearance, the system energy is described as:

$$V(\delta(t)) = \frac{M\dot{\delta}_T^2}{2} + \int_{\delta^0}^{\delta_T} P(u)du \tag{2.8}$$

The potential energy curve shown in Figure 2.2 helps in transient stability analysis. As the rotor angle reaches δ_{max}, the system becomes unstable such that if the fault is not cleared, the rotor angle trajectory will diverge towards δ^u. In a SMIB system, from Equation 2.5 and definition of PE_{max}, $V(\delta_T) < \mathrm{P}E_{max}$. Therefore,

$$\frac{M\dot{\delta}_T^2}{2} + \int_{\delta^0}^{\delta_T} P(u)du < \int_{\delta^0}^{\delta_u} P(u)du \tag{2.9}$$

Hence, the condition for stability is defined as follows:

$$P_m(\delta_T - \delta^0) < \int_{\delta_T}^{\delta_u} P(u)du \tag{2.10}$$

2.4 Summary

In this chapter, a review of power system stability problems is described in detail. The origin of the stability problems and the development of stability measures taken over the period of last century is being discussed. The adverse effects on the operation of power system due to instability and some of the major system collapses in history are specified in the first part of this chapter. The second section of the chapter discusses various transient stability analysis methods. The traditional methods which were used in the last century along with the changing approaches towards stability problems to meet the requirements of the complexity in the power systems were introduced in brief. Also, the recent methods involving data-driven techniques and machine learning algorithms is described and their shortcomings which are constantly overcome using the most advanced methods is brought to attention. The third section illustrates the formulations and mathematical modeling of the traditional techniques of transient stability analysis such as Lyapunov's method, EAC and TEF which were explained in detail.

Chapter 3: Online Transient Stability Assessment using Deep Learning CNN and HCP Approach

3.1 Introduction

In this chapter, a real-time framework is proposed for online monitoring of the power system transient stability. The proposed monitoring system utilizes available measurements—voltage and current magnitudes, voltage angle and frequency (rate of change of phase angle)—obtained from phasor measurement units (PMU) distributed across the grid. Using these measurements from PMUs, the measures for rotor angle can be easily estimated using various dynamic state estimation methods [118] . The deep learning network used in the proposed system is the convolutional neural network (CNN), which takes the heat-map representation of the aforementioned variables measured from PMUs and rearranged over a three-dimensional (3D) matrix as the input [143]. Each heatmap is a 3D matrix of the measured variables over a window of fixed length and the measurements are taken in overlapping time windows. The proposed network is a Y-net architecture [143] which detects the operating status of the system and the critical generators in case of unstable scenarios. This involves two different classifier networks, i.e., multi-class classification for predicting the state of the system and multi-label classification for identifying the critical generators. For the second multi-label classifier, a flexible hypotheses CNN pooling (HCP) [144] approach is proposed in which CNN outputs from different hypotheses are aggregated with max pooling to produce ultimate multi-label predictions to aggravate accurate identification of the system critical generators over all other previously proposed models. The performance of both proposed techniques is compared and the results are analyzed under different conditions in power system. The information obtained from the proposed deep learning framework can be used for planning mitigation strategies to arrest the propagation of the instability in interconnected power grids.

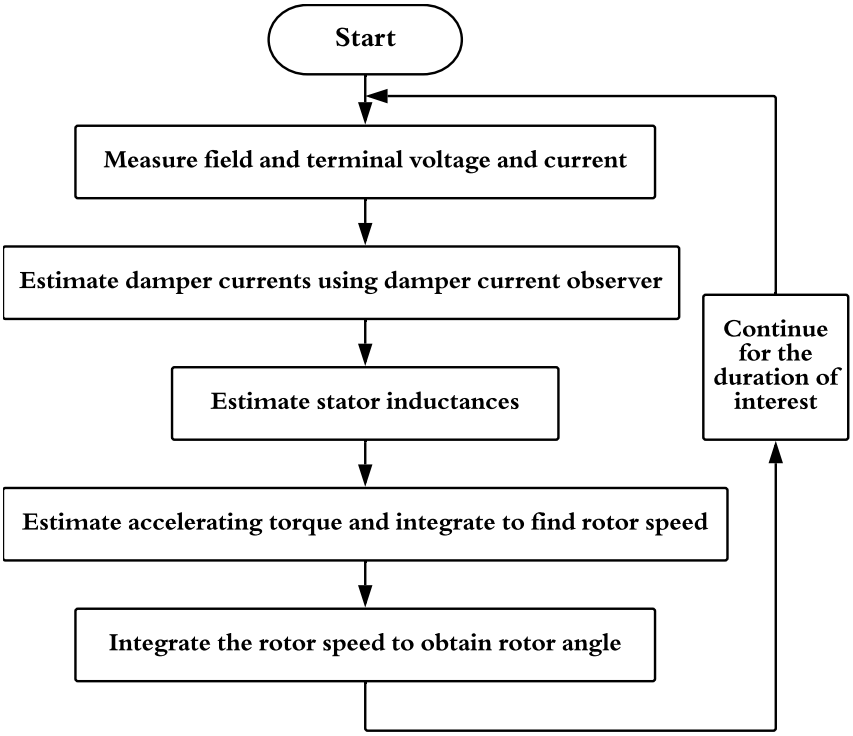

Figure 3.1: Rotor Angle Estimation Flowchart [5]

3.2 Rotor Angle Estimation

This chapter presents a method for rotor angle estimation using the measurements obtained from PMUs. In steady state condition, the rotor angle of the generator is directly available from its phasor diagram by using the current measurements and the terminal voltage [104, 145, 146]. However, during transient conditions, the reactances of the machine change their effective values and the estimation of the rotor angle from the PMU measurements is not straightforward as in the case of steady state conditions. There are various methods of estimating the rotor angle during transient conditions such as by solving dynamic equations of the machine [147], by estimating transient reactances from terminal measurements [148] etc. The rotor angle estimation method considered here is using the damper current measurements [5].

The process of rotor estimation method is described as shown in Figure 3.1. Once the fault takes place in the system, the estimation process is triggered and the process is

continued till the machine reaches the steady state operating condition.

The electrical torque of the generator machine is given by the equation below using the values L_d, L_q, i_D, i_Q, i_d, i_q and other known parameters of the machine [5].

$$T_e = (L_d - L_q) i_d i_q + k M_F i_F i_q + (k M_D i_q i_D - k M_Q i_d i_Q) \tag{3.1}$$

The swing equation of the generator is given by the equation below:

$$\frac{2H}{\omega_s} \frac{d\omega}{dt} = T_m - T_e = T_a \tag{3.2}$$

The accelerating or decelerating torque at the n^{th} instant on the rotor can be found from the equation below:

$$T_a(n) = T_m - T_e(n) \tag{3.3}$$

Using equation 3.3 in equation 3.2 and integrating it, the speed of the rotor can be calculated using the following equation,

$$\omega = \int \frac{T_a}{2H\omega_s} dt \tag{3.4}$$

The rotor angle can be obtained by integrating the speed of the rotor as follows,

$$\delta = \int (\omega - 1) dt \tag{3.5}$$

The above equation helps in estimating the rotor angle of the generator using PMU measurements during a transient condition (post disturbance).

3.3 Background on CNN and HCP Neural Network Models

Within the family of neural networks, and to train the data with grid-like topology such as images etc., deep CNN has been one of the greatest breakthroughs [149]. CNN consists of convolutional layer, pooling layer and fully connected layers (FCs). When applied

to single-label (multi-class) image classification, CNN can handle well-aligned images very well; however, for multi-label image classification, there arises complexity of miss-alignments and occlusion which would lead to relative inaccuracy in the prediction of such multi-label classification. On the other hand, HCP additionally consists of max pooling layer compared to CNN. It is a flexible deep CNN structure which can help alleviate these issues, since HCP takes segment hypotheses as the input which are generated by object detection techniques, and then connects a shared CNN to each hypotheses, finally aggregating single-label predictions from different hypotheses into the multi-label results [144].

A standard convolutional neural network for image recognition is shown in Figure 3.2. The input to the network is an image. The input layer is usually followed by convolutional layers [143]. Each unit in a convolutional layer is connected only to a few neighborhood neurons in the previous layer allowing for local connectivity [149]. The first convolutional layer consists of neurons which are meant for extracting some elementary features. The features extracted by convolutional layers are then combined by different higher layers to form complex features. In order to incorporate invariance to translations or distortions, all neurons in a convolutional layer share the same weights. This causes the same elementary feature detector to be applied across entire input image which is equivalent to convolution operation with a suitable-sized kernel. The output of such a set of units is called as feature map and the common weight vector is called a filter. Since units in a feature map extract similar features throughout the entire image, a convolutional layer is composed of several feature maps in order to extract multiple features from the image.

Typically, the features are extracted from the input data via the convolutional layer by the convolution kernel, defined by,

$$O_C^j = f\left(\sum_{i \in M_j} x_i * j_{ij} + b_j\right) \tag{3.6}$$

where O_c^j is the j^{th} feature map of the convolution layer, x_i is the input image set, k_{ij} is the

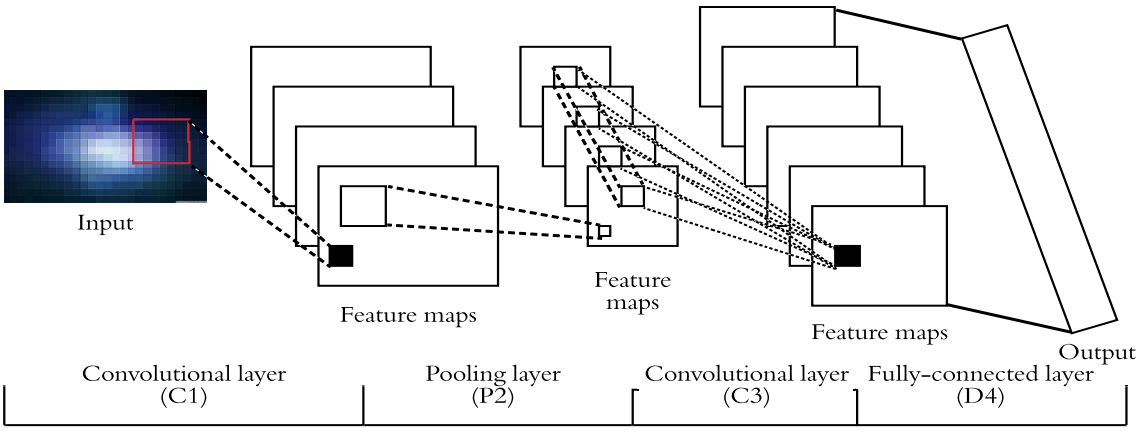

Figure 3.2: Architecture of a Standard CNN Model

convolution kernel corresponding to O_c and x_i, b_j is the bias. $*$ stands for the convolution operation and f is defined as $f = max\{0, x\}$.

The pooling layer extracts the important features from the convolutional layer, the output of which can be formulated as

$$O_P^j = f\left(\beta_j \text{down}(O_C^j) + b_j\right) \tag{3.7}$$

where *down* sampling function is represented and β_j is the j^{th} multiplier of the pooling layer. The fully connected layer may consist of multiple hidden layers and its output can be generally represented in the following form

$$\hat{y} = \sigma(wO_P + b_j) \tag{3.8}$$

where w is the weight and σ is the activation function. Suppose v_i is the output vector of the i^{th} hypotheses from the shared CNN and v_{ij} is the j^{th} component of v_i. The max pooling layer can be then formulated as

$$v^{(j)} = \max\left(v_1^{(j)}, v_2^{(j)}, \cdots, v_m^{(j)}\right) \tag{3.9}$$

where v_j can be considered as the predicted value for the j^{th} category of a given image.

For a multi-label classification, $y_i = [y_{i1}, y_{i2}, \cdots, y_{ic}]$ is the label vector of the i^{th} image. If the image is annotated with class j, then $y_{ij} = 1$ or else $y_{ij} = 0$. The probability vector for i^{th} image is defined as $\hat{p}_i = y_i/||y_i||$. The cost function to be minimized is then defined as

$$J = \frac{1}{M} \sum_{i=1}^{M} \sum_{k=1}^{c} (p_{ik} - \hat{p}_{ik})^2 \tag{3.10}$$

where M stands for the number of images.

The final output of the first classifier is obtained through a softmax operator. Softmax function calculates the estimated probability scores for each individual class. These scores are useful in deciding the most probable class for each input pattern. The activation function used at the output layer for the second classifier is the sigmoid function. In sigmoid activation function at the output layer, the neural network models probability of a class as a Bernoulli distribution. Sigmoid function [150], unlike softmax, does not give a probability distribution around different classes as the output, but provides independent probabilities. Multi-label classification tasks are not mutually exclusive and each class is independent; therefore, this function allows for such types of classifications.

The Adam optimizer is usually used to solve the CNN models and it obtains estimates of the first (m_t) and the second (v_t) order moments of the gradient as follows,

$$m_{t+1} = \beta_1 m_t + (1 - \beta_1) g_t \tag{3.11}$$

$$v_{t+1} = \beta_2 v_t + (1 - \beta_2) g_t^2 \tag{3.12}$$

where β_1, β_2 are user-defined constants and the estimates m_t, v_t are initialized by zero vectors. Assume g_t=g(θ_t) and let g_t^2 be the vector whose components are squares of components of g_t. These estimated moments are then used to update the parameters at time t as follows,

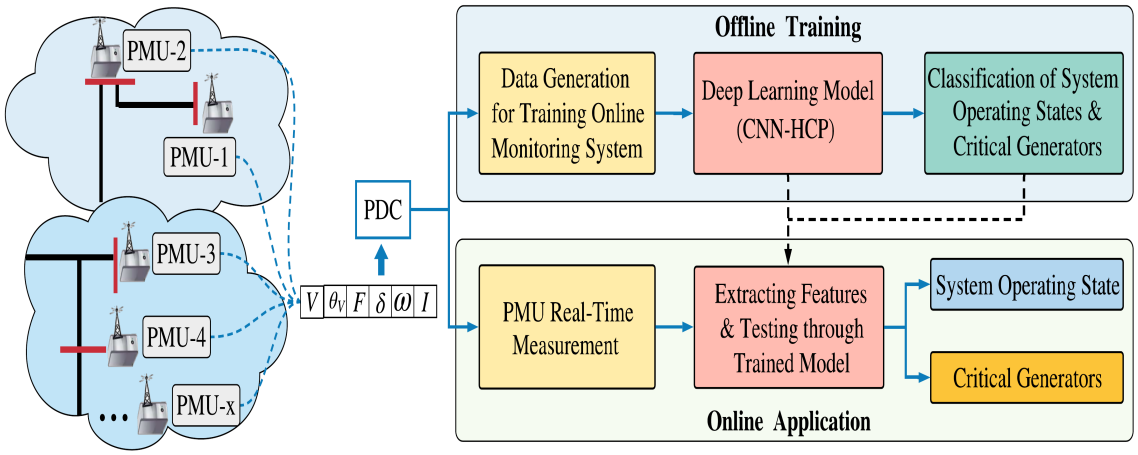

Figure 3.3: Proposed Framework for Power System Stability Surveillance using CNN-HCP

$$\theta_{t+1}^{i} = \theta_{t}^{i} - \frac{\eta}{\sqrt{v_t^i + \varepsilon}} m_t^i \tag{3.13}$$

where,

θ_t^i denotes the i^{th} parameter value at time t. m_t^i and v_t^i are the i^{th} components of the corresponding vectors.

3.4 Proposed Framework

The proposed framework for the case study in this chapter is illustrated in Figure 3.3. The application of the CNN model along with HCP network for detection of critical generators and operating states on the IEEE 118-bus test system is illustrated in this chapter. This chapter gives a detailed information about collection of data, pre-processing of data and application of the proposed deep learning neural network. The data obtained from PMUs is first used for offline training of the pre-built hybrid deep learning model. The trained model is then used for online assessment of the power system stability and to identify sets of critical generators in real-time. The results of the application of the proposed network for the given transient stability problem is explained towards the end of the chapter.

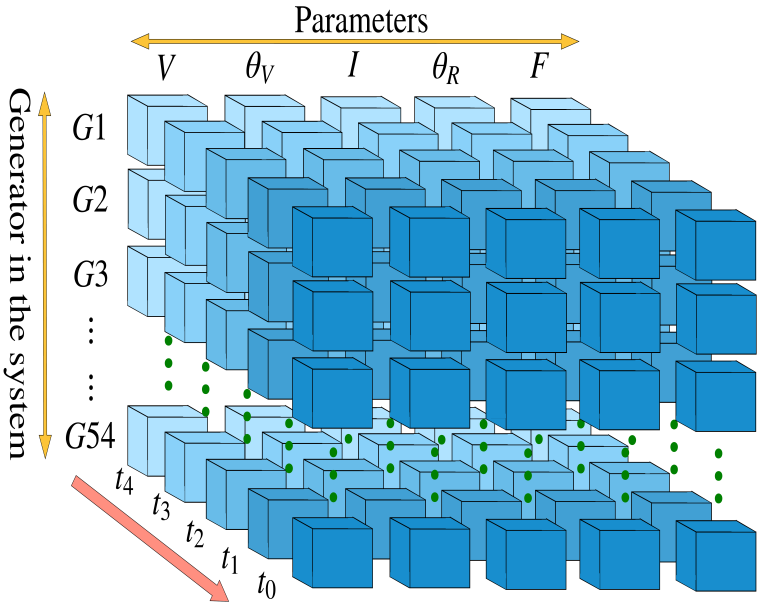

Figure 3.4: 3D Data Matrix Representation for CNN-HCP Model

3.4.1 Training Data Acquisition

The parameters used for training the model are the current and voltage magnitudes, rotor angle, voltage angle, and frequency. The training data is collected from PMUs located at all generator buses across the network, the data on which is obtained through TSA simulations on the IEEE 118-bus test system in the PowerWorld software environment. The IEEE 118-bus test system comprises of 118 buses, 54 generating units, 99 load points, and 177 transmission lines. The TSA simulations are conducted for various types of faults (3-phase balanced faults on each bus and on each transmission line at three different locations of 25%, 50% and 75% of the line length) and under varying loading conditions in the system.

Each simulation is run for a period of 20 seconds and a time-step of 0.02 seconds is used throughout, such that 1000 timestamp recordings are available for each contingency. For each contingency, the fault is created exactly at t = 1s and the fault is simulated for 8 cycles (i.e., 0.1333 seconds), after which it is cleared. All such contingencies including bus faults and transmission line faults are repeated for several load levels in the system (base load and -3%, -2%, -1%, +1%, +2%, +3%, +5% and 7%), for which the load flows are converged.

3.4.2 Data Pre-Processing

In order to monitor the system transient stability in real-time, the surveillance system needs to continuously analyze the power system parameters over few time-steps. All parameters described in Section 3.4.1 are observed over a sliding window of time stamps, lets say t time-stamps. Therefore, at every sampling instant, the sliding window consists of $(t-1)$ past measurement recordings and one current measurement recording. The observed raw data is rearranged and transformed into a three-dimensional vector (timestamp, generator number, parameter) as shown in Figure 3.4. There are 54 generators ($G1$ to $G54$) on *Generator* axis and 5 parameters in all on *Parameter* axis. Also, a range of timestamps exist on the *Time* axis. The length of each observation window is 5 timestamps and the sliding step is 1 timestamp.

A heat-map image of this three dimensional matrix is created for each sample, i.e., the data matrix for each sample is rendered a color image of size $T \times N \times P$, wherein T is the length of the observation window, N is the number of generators, and P is the number of parameters. Therefore, the size of each heat-map image for any particular fault scenario is considered constant and it is $5 \times 54 \times 5$. The representation of stable and unstable cases for bus and transmission line fault is shown in Figure 3.5. The demonstrated heat-maps are obtained by rearranging the data from 3D into a 2D matrix form (54×25) through stacking all 5 timestamps on the *parameter* axis.

3.4.3 Transient Stability Index

Transient stability assessment in power systems is captured using Transient Stability index (TSI). If a disturbance occurs and is cleared exactly after 8 cycles (t = 1.1333s), then the state of the system following the contingency can be theoretically determined via the TSI, which is defined as

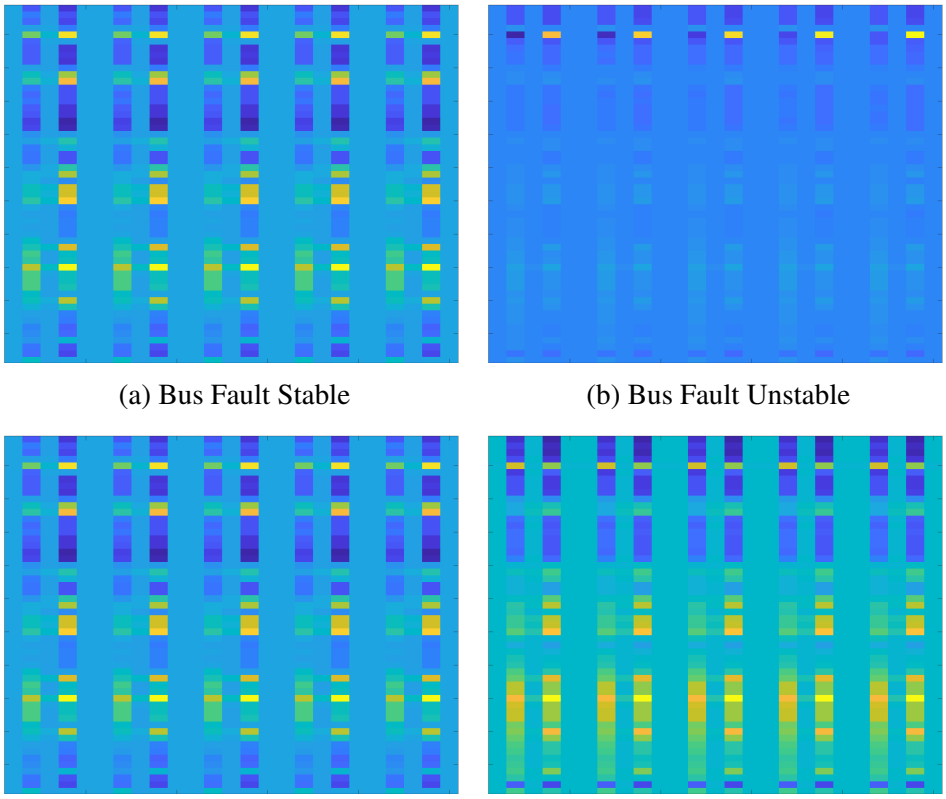

(a) Bus Fault Stable (b) Bus Fault Unstable

(c) Transm. line fault Stable (d) Transm. line fault Unstable

Figure 3.5: Visualization of the Extracted Features from Data Matrix in Stable and Unstable Cases for 118-Bus Test System.

$$\eta = \frac{360^\circ - |\Delta\delta|_{max}}{360^\circ + |\Delta\delta|_{max}} \tag{3.14}$$

where $\Delta\delta_{\text{max}}$ is the maximum rotor angle separation between any two generators following the fault. The system stability profiles obtained through the simulations are classified stable or unstable based on the value of η. A system is considered stable if $\eta > 0$, otherwise the system would be labelled as unstable. If a case is classified as an unstable case, and the angle separation of certain generators from the rest of the generators is more than 360°, then that set of generators is classified as critical for that particular contingency. The system operating states are distinguished into six different classes as shown in Table 3.1.

The system operating state is differentiated based on various events of interest taking

Table 3.1: Possible System State Labels based on Observed Data Matrices

Class 1 : No Disturbance	Class 4 : Fault Clearance
Class 2 : Fault Occurrence	Class 5 : Return to Stable State
Class 3 : Fault Duration	Class 6 : Unstable State

place in the system. A detailed description of these events and the classification of these six different classes are described as follows:

- ***Class 1:*** All the observed data matrices belong to the pre-fault operating time.
- ***Class 2:*** Any observed data matrix that covers the instant timestamp of the fault occurrence.
- ***Class 3:*** All the observed data matrices which cover exactly the timestamps that lie between fault occurrence and fault clearance (without instant timestamps of either fault occurrence or fault clearance).
- ***Class 4:*** Any observed data matrix which covers the instant timestamp of the fault clearance.
- ***Class 5:*** During post-fault clearance period, all the observed data matrices which reveal the stable state.
- ***Class 6:*** During post-fault clearance period, all the observed data matrices contain the instant timestamp of unstable states and all the timestamp afterward. Each data matrix is here associated with a set of critical generators.

The training data is generated following Section 3.4.1, and is classified and labeled accordingly based on Table 3.1. It is then used to train the deep learning model presented next.

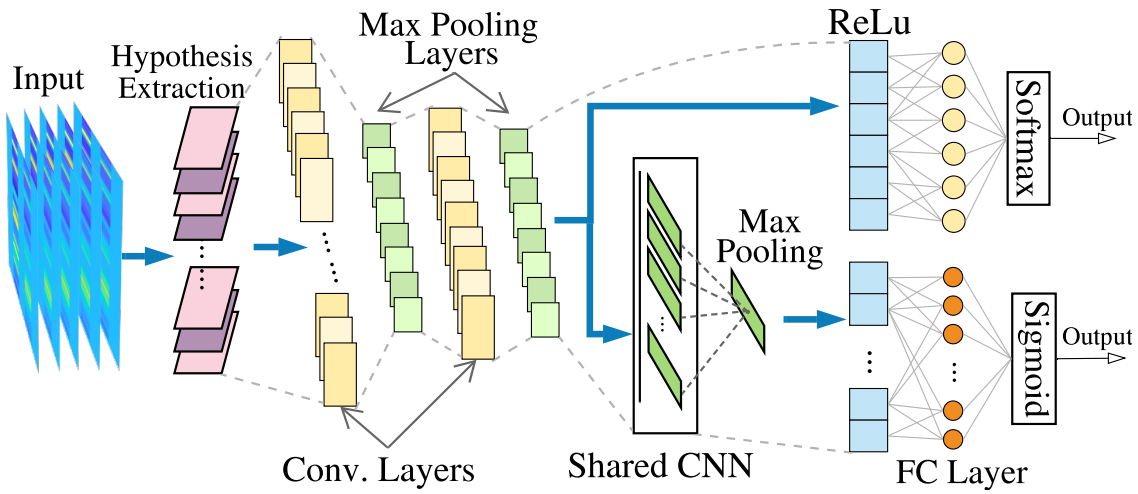

Figure 3.6: The Proposed CNN Architecture with Hypotheses Pooling

3.4.4 Proposed CNN-HCP Architecture

The suggested Y-net CNN architecture is shown in Figure 3.6, where firstly smaller candidate windows are selected within the input image as hypotheses by a hypotheses selection process. The selected hypotheses are fed into two convolutional layers to compress the split image into feature maps. After extraction of features from the data matrix, the network is divided into two different branches. The upper branch in the network, shown as Classifier 1, works as a multi-class classifier which detects the system stability. The lower branch shown as Classifier 2 performs a multi-label classification which identifies the system critical generators. Within Classifier 1, the extracted feature is fed into ReLu and fully connected layers, softmax is then used to give the output. For Classifier 2, the extracted feature acts as an input to the shared CNN and fuses individual hypotheses scores with a max pooling operation. Unlike Classifier 1, Classifier 2 uses a sigmoidal activation function. To integrate both branches, errors in both classifiers are back propagated together during the training process.

3.5 Numerical Results and Analysis

The IEEE 118-bus test system is used as the test platform, where a total of 5652 contingency scenarios are simulated including different types of faults under varying loading levels. The data set is randomly split into the training and validation test sets, and the represented results are averaged over these trials. The number of sample windows in ***Class 5*** (stable post transient disturbance) is much larger than the other classes, whereas, in ***Class 2***, ***Class 3*** and ***Class 4*** the number of samples is relatively lower. Hence, to balance the data for training the NN, sum-sampling is used to represent the data in equal proportions in the training dataset. Additionally, the input data for the training datasets in all the unstable cases of ***Class 6*** are modified to specify the indication of any critical generators in each particular unstable case. The performance of the proposed model has been tested under no noise consideration.

The implementation of the CNN algorithm is achieved in Tensorflow 1.14.0 with NVIDIA GeForce RTX, 64GB GPU (CUDA 10.0) support. The NN is trained with Adam Optimizer with a batch size of 64. The data matrix of the PMU readings generated through simulations in PowerWorld Simulator are used as the input to train the NN. The size of the input data matrix is very small (5x54x5)—the equivalent heat-map image size is (54x25)—compared to the normal image size (300x300) or (512x512). Therefore, while training the CNN module, a comparable image-size and a similar kernel size is used. The consideration of smaller image size works better as there is a need to look for global features in the data matrix and not local features. A similar kernel size to the size of the input image reduces additional computational burden.

In our online monitoring system, along with the accuracy of the model, another critical factor is the time taken for computation of the outputs in both introduced classifiers. The time required for computing the final output of a given sample window should be extremely low for the monitoring system to be considered viable in real-time applications.

The bar graph in Figure 3.7 represents the training time and the online monitoring time

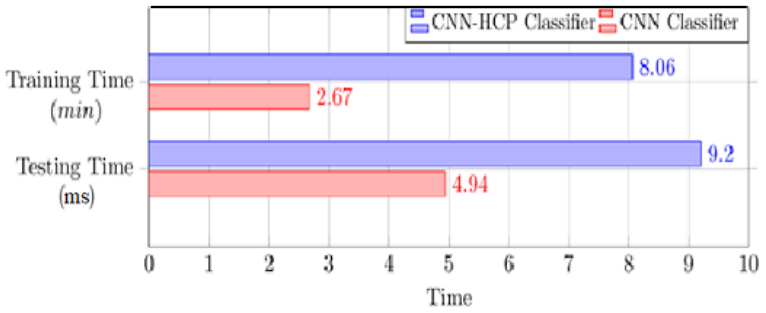

Figure 3.7: Training and Testing Time for CNN and CNN-HCP Models

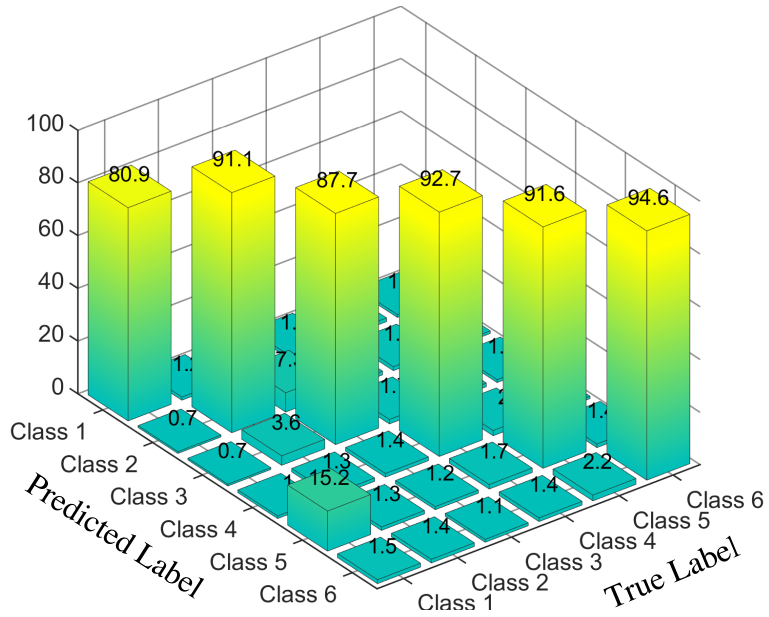

Figure 3.8: Confusion Matrix Representing Accuracy of the CNN-HCP Model

computed on two different models. The first model is the CNN model [149] (without HCP Framework) and the second model is the proposed flexible CNN-HCP framework used for detection of system critical generators. The time calculated for the final output of both models is 4.94*ms* and 9.2*ms*, respectively. Thus, although the proposed model is a bit slower in monitoring, it is still efficient enough to work in real-time. Furthermore, the training time for this model is relatively higher than that in traditional CNN model which is 2.67 minutes. The time required for training the proposed CNN-HCP network for the studied 118-bus test system is 8.06 minutes and the training is done offline.

The confusion matrix in Figure 3.8 shows the overall accuracy in detecting the system operating state for different load conditions during the testing process. For each class, 3000 samples are taken for testing purposes. The labels in the *True Label* stand for the true class of the testing data and the *Predicted Label* stands for the classified results of the CNN-HCP model. As the result shows, 91.1% samples are correctly classified to detect ***Class 2*** and 1.4% of the samples are mistakenly classified as ***Class 6***.

The greater training and testing time comes with an increased accuracy rate for the suggested hybrid model in this chapter. The bar graph in Figure 3.9 represents a similar accuracy rate for classifying the state of the system and a considerable increase in accuracy rate while detecting the critical generators when the system is trained for the entire dataset (including all types of faults at all varying load conditions specified in Section 3.4.1). Secondly, the proposed model is tested on the base and varying load conditions separately and compared with the CNN model in [149]. In all the given test cases, the results represent that the suggested CNN-HCP model outperforms in all conditions as compared to the previously studied CNN model in [149] which does not use the HCP framework for multi-label classification. For the base case load, when trained for 3-phase faults on buses and transmission lines at three different locations, the total number of 628 contingencies are considered. For the varying load conditions ($\pm$2 and 3%), a total number of 2512 contingencies are modeled for training, which includes all different types of faults. In both load conditions, the results of the Classifier 1 obtained from both frameworks reveal a similar accuracy rate. However, the accuracy rate of Classifier 2 from the proposed framework shows a significant improvement, compared with that from [149], which verifies that the proposed framework can be more robust when it comes to detecting the set of critical generators in power systems following a transient disturbance.

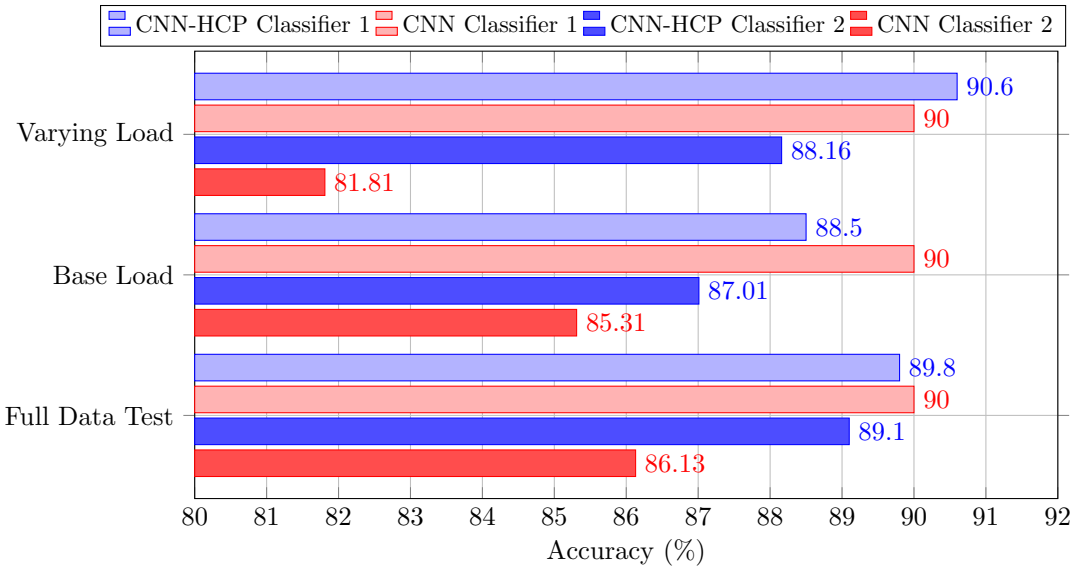

Figure 3.9: Detection Accuracy at Base Load and Varying Load Conditions

3.6 Summary

This case study presents an advanced deep learning framework for online detection of unstable operating states in power systems and real-time identification of system critical generators following disturbances. The proposed framework utilizes phasor measurements from PMUs at the generator buses and classifies the events based on the features extracted from the measurements. In the proposed framework, CNN is used to classify two different outputs simultaneously, which consists of multi-class and multi-label classifications, followed with a suggested HCP technique for the latter classification. The performance of the proposed framework is tested on a variety of scenarios and under varying load conditions. Simulations verified that the proposed framework with HCP reveals a more accurate outcome compared to the traditional CNN models. The suggested model comes with a higher accuracy at the trade off of the computing time, yet computationally-efficient and applicable to applications in online setting.

Chapter 4: Online Transient Stability Assessment Using a Hybrid Deep Learning Convolutional LSTM framework

4.1 Introduction

This chapter gives an insight on the real-time monitoring of the power systems transient stability using a different deep learning approach along with developments to the framework in terms of robustness to a variety of fault conditions and advancements in the data used for training the online monitoring model. Similar to the previous model, the work proposed in this chapter for real-time monitoring utilizes measurements available from PMUs located at each generator buses, including voltage, current, voltage angle and frequency. In addition to the measurements obtained from PMUs, rotor angle values are calculated using the dynamic state estimation methods and the available measurements. Additionally, a new system variable in the form of rotor speed is also added to the data set in the following work. The addition of a new system variable to the data set will improve the potentials of the deep learning neural network to extract additional features from the data while training the model. The deep learning network used in the proposed study is the Convolutional Long-short term memory (LSTM) network, which takes a heat-map representation similar to the one in the previous chapter but with addition of a sixth variable to the heat-map data from the PMUs and rearranged over a 3D matrix as the input. Each heatmap is a 3D matrix of the measured (and estimated) variables over a window of fixed length and the measurements are taken in overlapping time windows. The proposed deep learning neural network in this chapter is a dual output problem detecting the operating state and the critical generators in the system. Therefore, a Y-net architecture with two outputs, one as the multi-class classifier and the second one with multi-label classifier, is used. For the time-series characterized data, an interesting approach is to use a model based on the LSTM architecture. The output of the Convolutional LSTM layer, which is a recurrent

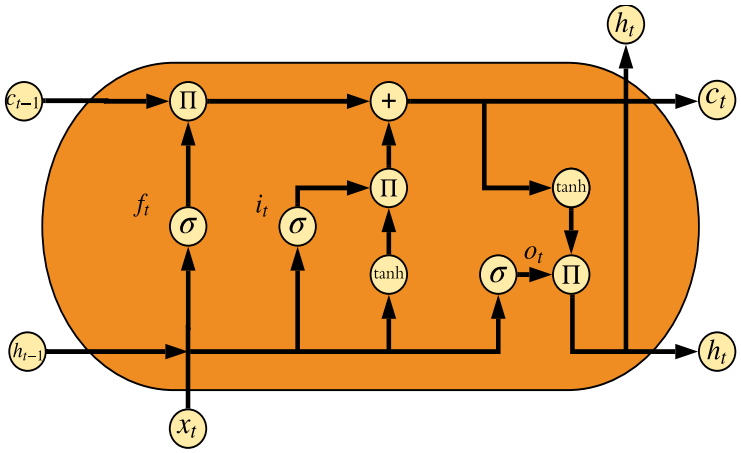

Figure 4.1: Basic Structure of the LSTM Cell

layer is a combination of a Convolutional and the LSTM output, wherein the internal matrix multiplications are replaced by convolutional operations unlike LSTM layers [151]. The performance of the proposed technique in this chapter is compared with previous models and results are analyzed under different fault conditions in the power system. The advanced deep learning framework can be utilized by the independent system operator to ensure an uninterrupted operation of the grid and for planning mitigation strategies in facing with the instability scenarios.

4.2 Background on ConvLSTM Neural Network

Xingjian Shi introduced the Convolutional LSTM (ConvLSTM) as a variant of LSTM in 2015 [152] to learn spatial information in the dataset. To learn ConvLSTM, it is important to know a brief insight of LSTM networks. For sequence modeling, LSTM has been proven stable and powerful for modeling long-range dependencies due to its nature as a special RNN structure [153–156]. Figure 4.1 [157] shows the basic structure of the LSTM cell with input gate i_t, output gate o_t, forget gate f_t and final state h_t. The memory cell c_t in a LSTM network acts as an accumulator of state information. The controlling gates help in accessing, writing and clearing information in a cell. For a new input instance, the information of the incoming input gets accumulated in the cell only if the input gate i_t is activated. In case the

forget gate f_t is on, the past cell c_t information will be forgotten in the process. The new incoming cell is propagated to the final state h_t and it is controlled by the output gate o_t.

The use of cell and gates to control information flow is advantageous as it prevents the gradient from vanishing too quickly by trapping it in a cell. The formulations of a version of LSTM called fully-connected LSTM (FC-LSTM) with input, cell output and final state in 1D vectors are shown below [153]. Here, "$\circ$" denotes the Hadamard product:

$$i_t = \sigma(W_{xi}x_t + W_{hi}h_{t-1} + W_{ci} \circ c_{t-1} + b_i) \tag{4.1}$$

$$f_t = \sigma(W_{xf}x_t + W_{hf}h_{t-1} + W_{cf} \circ c_{t-1} + b_f) \tag{4.2}$$

$$c_t = f_t \circ c_{t-1} + i_t \circ tanh(W_{xc}x_t + Whch_{t-1} + b_c) \tag{4.3}$$

$$o_t = \sigma(W_{xo}x_t + W_{ho}h_{t-1} + Wco \circ c_t + b_o) \tag{4.4}$$

$$h_t = o_t \circ tanh(c_t) \tag{4.5}$$

The FC-LSTM network has proven to produce good results over the years, but it also has some drawbacks and problems of redundancy for the data. To overcome the drawbacks of FC-LSTM, an extension to it containing convolutional structures in input-to-state and state-to-state transitions was proposed in [152]. The usage of full connections in input-to-state and state-to-state transitions of FC-LSTM is its major drawback. The ConvLSTM determines the future state of a certain cell in the grid through its local neighbour's inputs and past states [152]. The formulations related to the ConvLSTM network are given in the equations below:

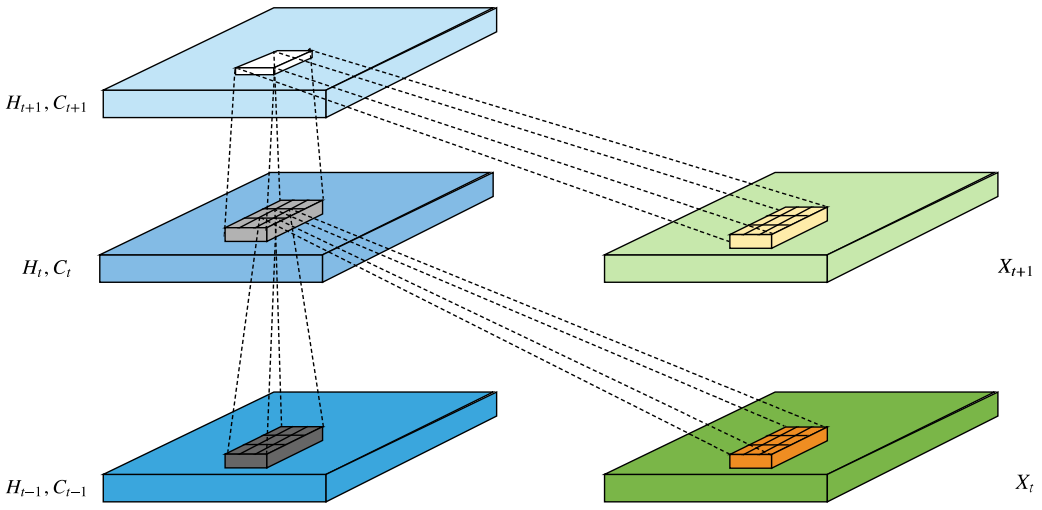

Figure 4.2: Inner Structure of the ConvLSTM

$$i_t = \sigma(W_{xi} * X_t + W_{hi} * H_{t-1} + W_{ci} \circ C_{t-1} + b_i) \tag{4.6}$$

$$f_t = \sigma(W_{xf} * X_t + W_{hf} * H_{t-1} + W_{cf} \circ C_{t-1} + b_f) \tag{4.7}$$

$$C_t = f_t \circ C_{t-1} + i_t \circ tanh(W_{xc} * X_t + W_{hc} * H_{t-1} + b_c) \tag{4.8}$$

$$o_t = \sigma(W_{xo} * X_t + W_{ho} * H_{t-1} + W_{co} \circ C_t + b_o) \tag{4.9}$$

$$H_t = o_t \circ tanh(C_t) \tag{4.10}$$

where "$*$" denotes the convolutional operator, X_1,...,X_t are the inputs, C_1,...,C_T are the cell outputs, H_1,...,H_t are the hidden states and i_t, f_t, o_t are the input, forget and output gates, respectively. The main difference between the FC-LSTM and ConvLSTM is the number of input dimensions [158]. FC-LSTM is better suited for one-dimensional data as the input and ConvLSTM is designed for three-dimensional input data. The difference in the formulations of FC-LSTM and ConvLSTM is the convolutional operation ($*$) which is substituted for the matrix multiplication. ConvLSTM is composed of similar convolutional structures as in the operation of CNN; however, its special internal design makes it possible to capture

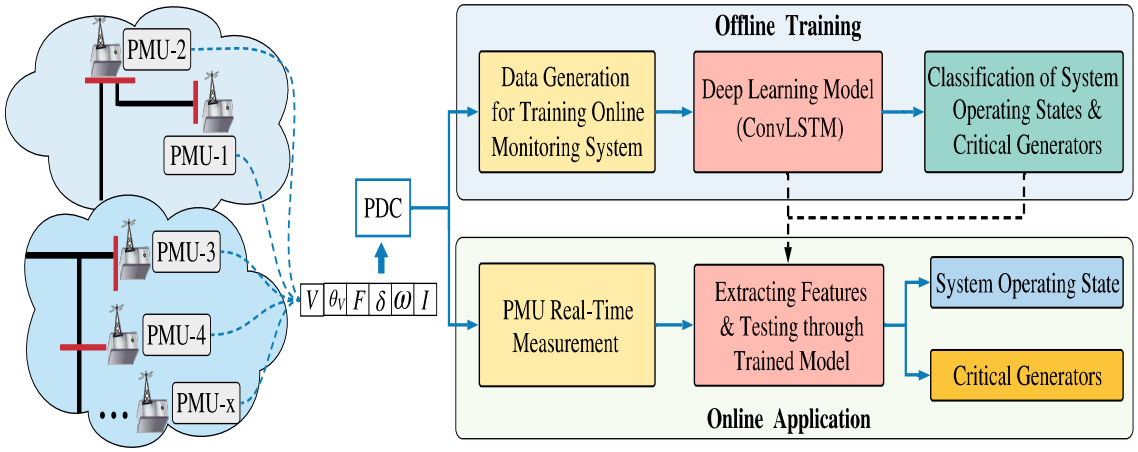

Figure 4.3: Proposed Framework for Power System Stability Surveillance using ConvLSTM

information from the input easier into its memory cells [159].

The inner structure of the ConvLSTM is shown in Figure 4.2 [152]. The 3D data with a size of T x N x P is given as the input to each memory cell in the ConvLSTM. There are three special gate units as shown, which makes it possible to extract more discriminating feature representation for a classification problem [159]. The convolutional kernel for 2D and 3D ConvLSTM differs as 2D input has convolutional filter with k x k kernel in the cell while the 3D input has a convolutional filter with k x k x d as the kernel, where "k" is the kernel size and "d" is the depth of the convolutional filter.

4.3 Proposed Framework

The proposed framework for the second case study is illustrated in Figure 4.3. In this chapter, a case study on the IEEE 39-bus test system has been carried out using an advanced Hybrid Deep Learning ConvLSTM model for detection of operating state and critical generators during a transient disturbance. Further, the chapter explains the process of data-collection and data cleaning; and a detailed description of the proposed deep learning neural network on the generated datasets. Compared to the proposed model in the last case study, this study has a similar set-up of three different steps viz. data collection, offline training, and online application. The results of the application of the upgraded neural network model for the

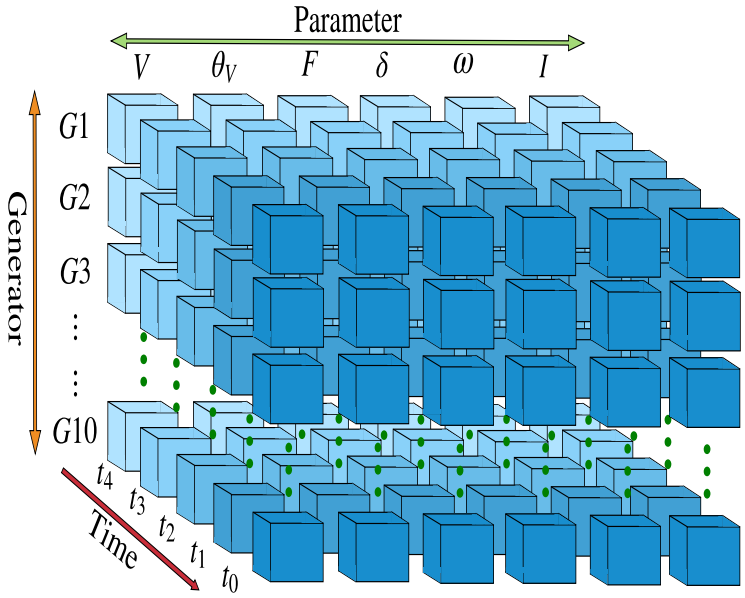

Figure 4.4: 3D Data Matrix Representation for ConvLSTM Model

given transient stability problem is explained in the later stage.

4.3.1 Training Data Acquisition

The parameters used for training the model are the voltage magnitude (V), voltage angle (θ_V), rate of change of phase angle i.e. frequency (F), rotor angle (ω), rotor speed (δ) and current magnitude (I). The training data is collected from PMUs located at all generator buses across the network, the data set which is obtained through TSA simulations on the IEEE 39-bus test system in the PowerWorld software environment. The IEEE 39-bus test system comprises of 39 buses, 10 generating units, 31 load points, and 46 transmission lines. The TSA simulations are conducted for various types of faults: 3-phase balanced faults on each bus and on each transmission line at 50% of the line length and under varying loading conditions in the system. In this study, dual contingencies in the system are also considered such as faults on 2 elements in the system. All combinations of either bus and transmission line or any two transmission lines in the system are considered to train the neural network to detect the critical generators in case of instability.

For the given case study in this chapter, six system variables are used as compared to five in the last test case. Four of which are directly obtained from the PMUs and the other two viz. rotor angle and rotor speed, are assessed using the dynamic state equations. The formulations for rotor speed and rotor angle using the damper current measurements are given in Section 3.2. Rotor speed can be calculated using Equation 3.4 and rotor angle can be calculated integrating the equation for rotor speed shown in 3.5.

Each simulation is run for a period of 20 seconds and a time-step of 0.02 seconds is used throughout, such that 1000 timestamp recordings are available for each contingency. For each contingency, the fault is created exactly at t = 1s and the fault is simulated for 8 cycles (i.e., 0.1333 seconds), after which it is cleared at t = 1.1333s. All such contingencies including bus faults and transmission line faults are repeated for several load levels in the system (base load, +1%, +3%, +5% and +7%), for which the load flows are converged.

4.3.2 Data Pre-processing

In order to monitor the system transient stability in real-time, the surveillance system needs to continuously analyze the power system parameters over few time-steps. All parameters described in Section 4.3.1 are observed over a sliding window of time stamps, lets say t time-stamps. Therefore, at every sampling instant, the sliding window consists of $(t-1)$ past measurement recordings and one current measurement recording. The observed raw data is rearranged and transformed into a three-dimensional vector (timestamp, generator number, parameter) as shown in Figure 4.4. There are 10 generators ($G1$ to $G10$) on *Generator* axis and 6 parameters in all on *Parameter* axis. Also, a range of timestamps exist on the *Time* axis. The length of each observation window is 5 timestamps and the sliding step is 1 timestamp.

A heat-map image of this three dimensional matrix is created for each sample, i.e., the data matrix for each sample is rendered a color image of size $T \times N \times P$, wherein T is the length of the observation window, N is the number of generators, and P is the number of

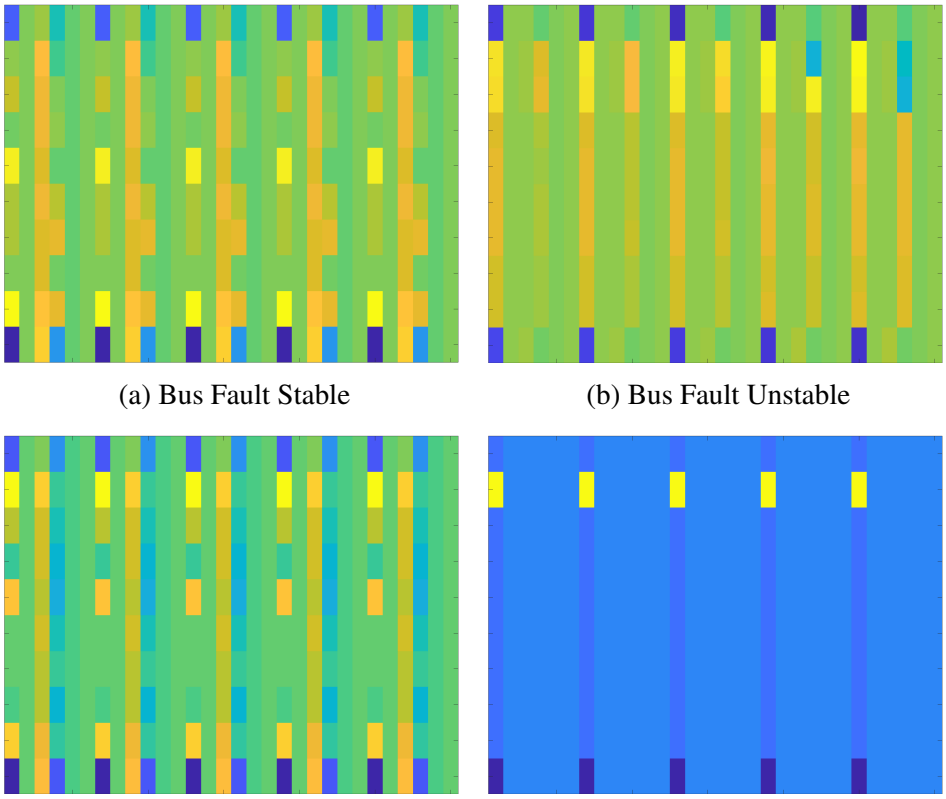

(a) Bus Fault Stable (b) Bus Fault Unstable

(c) Transmission line fault Stable (d) Transmission line fault Unstable

Figure 4.5: Visualisation of the Extracted Features from Data Matrix in Stable and Unstable Cases for 39-Bus Test System

parameters. Therefore, the size of each heat-map image for any particular fault scenario is considered constant and it is $5\times10\times6$. The representation of stable and unstable cases for bus and transmission line fault is shown in Figure 4.5. The demonstrated heat-maps are obtained by rearranging the data from 3D into a 2D matrix form (10×30) through stacking all 5 timestamps on the *parameter* axis.

The formulation equation for transient stability index used is the same as given in Equation 3.14. The distribution of operating states before and after the clearance of a transient disturbance in the system is given in Table 3.1. The description of each of the six different operating classes is taken as described in Section 3.4.4. The training data generated follows the formulation and segregation of classes as mentioned in the last chapter. Thereafter, it is used to train the proposed deep learning neural network.

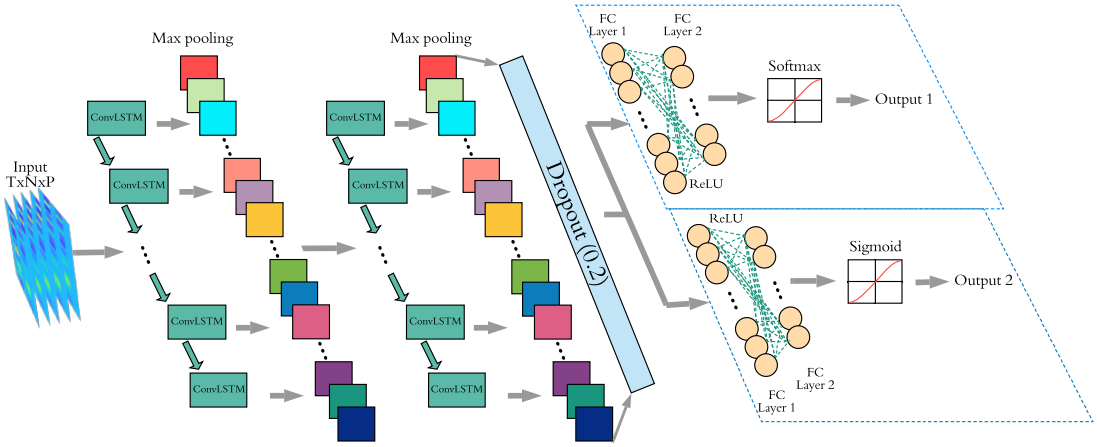

Figure 4.6: The Proposed ConvLSTM Architecture

4.3.3 Proposed Hybrid ConvLSTM Architecture

The suggested ConvLSTM architecture with a Y-net structure is shown in Figure 4.6. It is evident from the figure that the heatmap input is firstly passed through ConvLSTM layer in which valuable information from the input data is extracted in each of the ConvLSTM cells. The extracted features from the input data are fed through max pooling layer to reduce the spatial size of the data representation and computations in the network. The max pooling layer operates on each feature map independently. Further, the input is fed through another set of ConvLSTM and max pooling layers before passing through the dropout layer which is used to prevent the model from over-fitting. Dropout layer forces the network to learn more robust features and almost doubles the number of iterations required for the model to converge [160]. However, the time taken for training each epoch is lessened.

On extraction and reduction of features from the data matrix, the network is divided into two branches to form a Y-net structure. Since the case study focuses on detecting operating state and critical generators, a multi-output network is expected in the form of Y-net structure. The upper branch in the network, producing output 1, works as a multi-class classifier which detects the system stability. The lower branch producing output 2 performs a multi-label classification which identifies the system critical generators. In case of both

the classifier branches, the output from the dropout layer is fed into multiple fully connected layers and ReLU activation function. The fully connected layer represents feature vector of the input. This feature vector consists of vital information which is important to classify the features from the input data matrix. The ReLu is the max function with input data X which can be represented as [161]:

$$ReLU(x) = max(0,x) \tag{4.11}$$

By the use of ConvLSTM and max pooling layers, valuable features extracted are fed to the classification layers to predict the conditional probability distribution as given below [159]:

$$P(y = i|x,W,b) = \frac{e^{(W_{ix}+b)}}{\sum_{j=1}^{N}(e^{(W_{jx}+b)})} \tag{4.12}$$

where W is the weight and b is the bias of the classification function. Additionally, the final classification result is obtained from cross entropy used as the loss function described below:

$$L_{loss}(Y,\tilde{Y}) = -\sum(Y \cdot log(\tilde{Y})) \tag{4.13}$$

where Y is the ground truth and $\tilde{Y}$ is the corresponding predictive value of the proposed deep model. For optimization of the loss function, Adam optimizer is used to obtain the probability value of each pixel.

4.4 Numerical Results and Analysis

The IEEE 39-bus test system is used as the test platform, where a total of 16,200 contingency scenarios are simulated including different types of faults under varying loading levels. In the previous case study, only single contingency analysis i.e. disturbances at only one element in the system at any given time were considered and the model was trained for the generated single contingency fault scenarios. However, in the current study of 39-bus test system, along with the fault scenarios at single elements, cases of occurrence of faults

at two elements in the system is also considered and the model is trained accordingly for dual contingency scenarios. The entire data consisting of single and dual fault contingency scenarios is obtained by simulations in the PowerWorld software environment. The data set is randomly split into the training and validation test sets, and the represented results are averaged over these trials. The number of sample windows in ***Class 5*** (stable post transient disturbance) is much larger than the other classes, whereas, in ***Class 2***, ***Class 3*** and ***Class 4*** the number of samples is relatively lower. Hence, to balance the data for training the neural network, sum-sampling is used to represent the data in equal proportions in the training dataset. Additionally, the input data for the training datasets in all the unstable cases of ***Class 6*** are modified to specify the indication of any critical generators in each particular unstable case. The performance of the proposed work has been tested under no noise consideration.

The proposed model is trained with Adam Optimizer with a batch size of 512. The size of the training data in mat files is nearly 9.12GB. The training epoch used is 100; and it took about 12h to learn from the data (for ConvLSTM). Jaccard Accuracy is used to measure the predicted accuracy of the training case and the test case in real-time. The implementation of the ConvLSTM algorithm is achieved with the following configurations:

- CPU: Intel® Core^{TM} i9-9900 Processor @ 5.00 GHz.
- RAM: 64GB 2133MHz DDR4 ECC Reg.
- GPU: Nvidia GEFORCE RTX 2080 Ti @ 14000 MHz
- SSD: 2Tb 3D TLC NAND flash @ upto 500k IOPS
- Framework: Tensorflow 1.14.0, Python 3.7

The data matrix of the PMU readings generated through simulations in PowerWorld Simulator are used as the input to train the neural network. The size of the input data matrix is very small (5x10x6)—the equivalent heat-map image size is (10x30)—compared to the normal image size (300x300) or (512x512). Therefore, while training the CNN module,

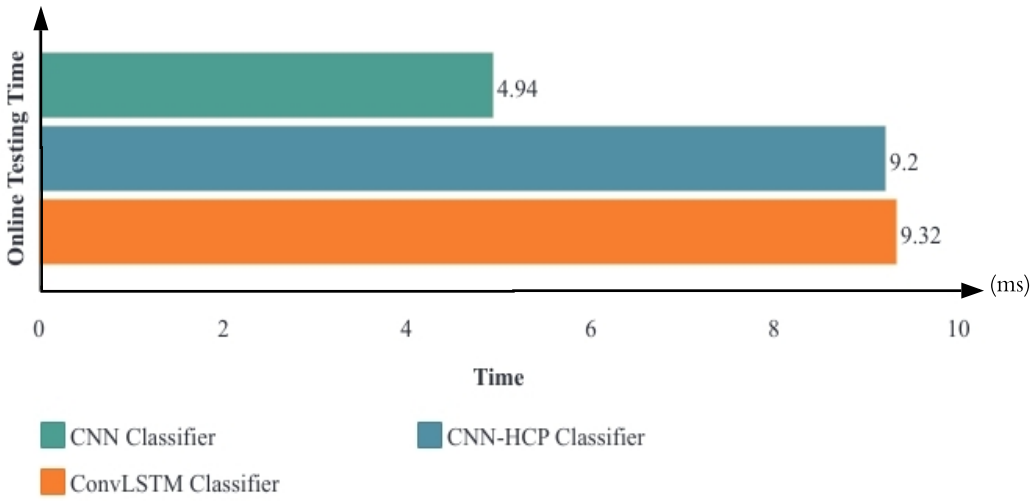

Figure 4.7: Comparison of Online Testing Time for CNN, CNN-HCP and ConvLSTM Models

a comparable image-size and a similar kernel size is used. The consideration of smaller image size works better as there is a need to look for global features in the data matrix and not local features. A similar kernel size to the size of the input image reduces additional computational burden.

In our online monitoring system, along with the accuracy of the model, another critical factor is the time taken for computation of the outputs in both introduced classifiers. The time required for computing the final output of a given sample window should be extremely low for the system to be considered viable in real-time.

The bar graph in Figure 4.7 represents the online monitoring time computed on two different models. The first model is the standard CNN model [149] with convolutional and pooling layers, the second model is the flexible CNN-HCP framework proposed in the previous chapter used for detection of system critical generators and the third model is using the hybrid ConvLSTM network with LSTM layers combined with convolutional computations for better accuracy. The time calculated for the final output of all three models are 4.94*ms*, 9.2*ms* and 9.32*ms*, respectively. Thus, although the proposed ConvLSTM model is slightly slower in monitoring, it is still efficient enough to work in real-time. Due to

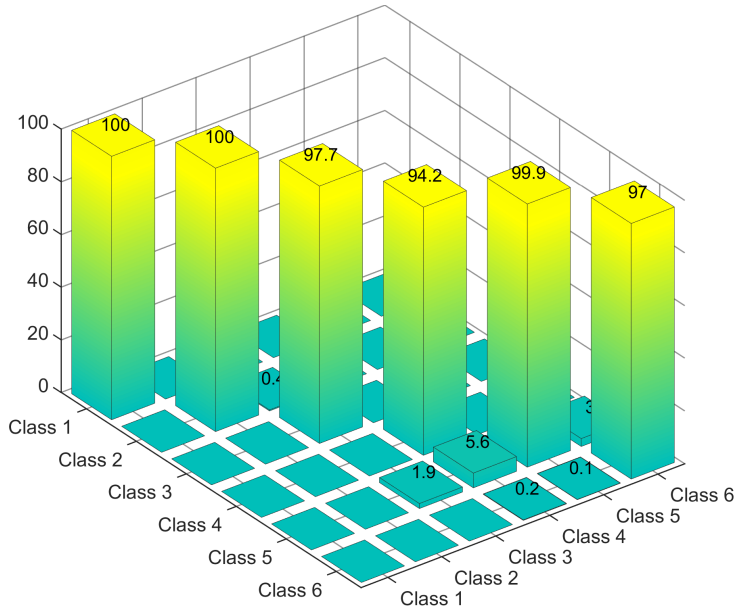

Figure 4.8: Confusion Matrix Representing Accuracy of the ConvLSTM Model

the inclusion of data scenarios wherein consideration of faults at dual elements at a time is taken into account, the enormous data leads to higher training time as compared to the other models. However, since the training of the model is done offline, it does not affect the online monitoring system as the proposed model detects the output in 9.32*ms* which is much lower than the time-step of 0.02s considered for each fault case.

The confusion matrix in Figure 4.8 shows the overall accuracy in detecting the system operating state for different load conditions during the testing process. For each class, 3000 samples are taken for testing purposes. The labels in the *True Label* stand for the true class of the testing data and the *Predicted Label* stands for the classified results of the CNN-HCP model. As the result shows, 100% samples are correctly classified to detect ***Class 1*** and ***Class 2***; whereas 97.7% samples are correctly classified to detect ***Class 3*** and 1.9% of the samples are mistakenly classified as ***Class 5***. Similarly, 99.9% and 97% samples are correctly classified to detect ***Class 5*** and ***Class 6*** respectively; 0.1% of the samples are mistakenly classified as ***Class 6*** instead of ***Class 5*** and 2.9% of the samples are mistakenly classified as ***Class 5*** instead of ***Class 6***.

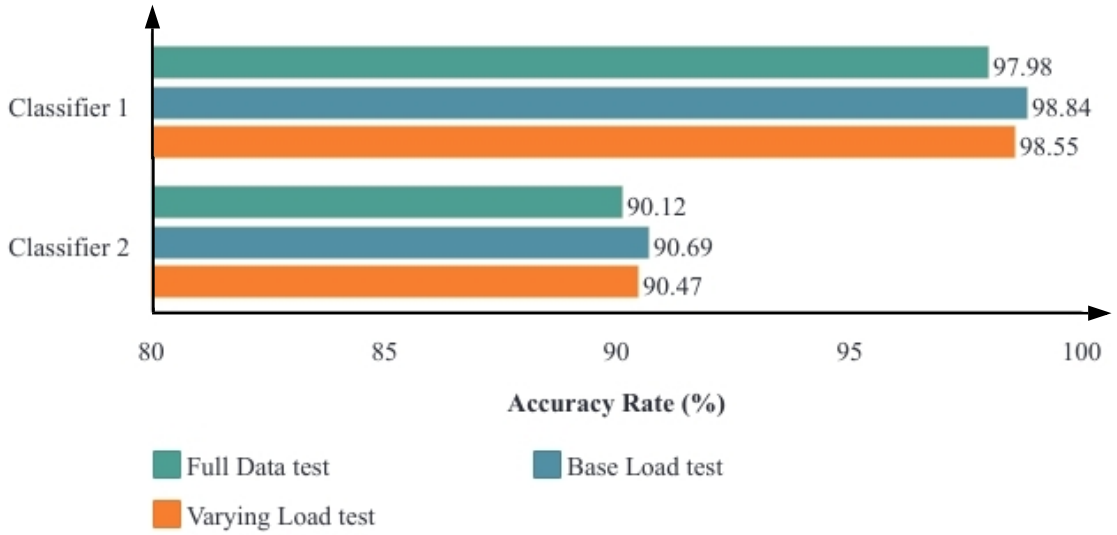

Figure 4.9: Detection Accuracy Rate at Different Load Levels using the ConvLSTM Model

The greater training and testing time comes with an overly increased accuracy rate for the suggested hybrid model in this chapter. The bar graph in Figure 4.9 represents an improved accuracy rate of about 98 % for classifying the system operating state and an increased accuracy rate of over 90% for detecting the set of critical generators for all test cases when the system is trained for the entire dataset (including all types of faults at all varying load conditions specified in Section 4.3.1). The proposed model is tested separately for base case load condition, varying load condition and also with consideration of entire data together including base case and varying load levels. As compared to the results in the previous chapter, the ConvLSTM model proposed in this chapter outperforms all the other deep learning techniques applied for power system stability monitoring. For the base case load, when trained for 3-phase faults on buses and transmission lines at center of the line length, and combination of faults on two elements in the system, the total number of 3240 contingencies are considered. For the varying load conditions (1%, 3%, 5% and 7%), a total number of 12,960 contingencies are modeled for training, which includes all different types of faults. The results for base case load and varying load levels differ slightly, but for all the cases shown in Figure 4.9, the accuracy rates are similar. For both classifier outcomes,

the proposed framework shows a significant improvement compared to the other models discussed in the Chapter 3. The discussion of the proposed framework and its results verify that the ConvLSTM model can be more robust and reliable when it comes to monitoring the power system stability following a transient disturbance.

4.5 Summary

This case study presents an advanced ConvLSTM deep learning framework for online detection of unstable operating states in power systems and real-time identification of system critical generators following disturbances. For the study discussed in this chapter, measurements from PMUs are utilized and the features from the PMU data are extracted to classify events based on the classes described in Section 3.4.4. In the proposed framework, ConvLSTM layers along with max pooling layers are used to extract valuable features from the data matrix and the extracted features are passed through classification layers like fully connected layers and ReLU activation function. The performance of the proposed framework is tested on a variety of scenarios and under varying load conditions. Simulations verified that the proposed framework with a hybrid deep learning model reveals a more accurate outcome compared to all the applied models. The suggested model comes with a higher accuracy at the trade off of the computing time, yet computationally-efficient and applicable in online settings.

Chapter 5: Conclusion

5.1 Concluding Remarks

Online monitoring of the power grid stability is crucial for operation of liberalized and integrated modern-world power systems where the system experiences greater uncertainties and fluctuations compared to the past. There is a dire need for fast and effective tools for power system stability surveillance against different types of instability problems the system may go through. Enhancement of the power system stability assessment methods in a modernized power system is much needed. Therefore, the research demonstrated in this thesis provides an effective way of assessing transient stability in power grids in real-time using the advanced deep learning neural network tools. The proposed methodology is based on two different deep learning models. During an instability condition in the system, the possibility that a generator machine goes out of synchronism increases. For a particular disturbance occurring in the system, one or more than one generator machine in the system may be severely disturbed and run out of synchronism. Hence, along with monitoring the system stability, identification of the set of critical generators that are severely disturbed is necessary to be assessed. Therefore, the study in this thesis not only provides a model for monitoring the system operating states, but also a tool for online detection of system critical generators in case of transient disturbances.

The thesis includes two case studies with two different deep learning models implemented on two different IEEE test systems in order to verify the results as compared to the state-of-the-art models. An upgrade over the previous approach of using heat-maps for the purpose of power system stability surveillance has been demonstrated by using detailed information of the system variables for more robust and accurate monitoring results. The study presented in this thesis utilizes additional system variables to build a robust model which yields more accountable outcome. The use of advanced hybrid deep learning models

viz. CNN with HCP (for improved multi-label classification of critical generators) and ConvLSTM (use of convolutional computations in LSTM layers) has been accomplished for the proposed problem.

The first case study utilizes deep learning CNN algorithm with hypotheses pooling on an IEEE 118-bus test system and the numerical results are discussed and verified by comparing with the traditional CNN method in Chapter 3. The second case study is implemented on an IEEE 39-bus test system using the hybrid deep learning algorithm which utilizes CNN and LSTM methods called ConvLSTM network and the numerical results are presented in Chapter 4. The proposed neural network models can be utilized to make the power grid more stable and robust against large disturbances. The proposed online stability monitoring tools can help to determine the abnormal operating conditions and unstable generator machines in real-time.

5.2 Future Work

The extension of the project could be to implement the work on a larger real-world power grid to test the variations in the results accuracy and computational effectiveness for real-time applications. The advancements in the field of neural networks and deep learning are moving at a rapid pace; therefore, the next step could be to use an advanced deep learning algorithm which could process the images to train the model for better accuracy and faster monitoring of the system. Current work trains the deep learning models offline based on the historical data which could be applicable in real-time. However, a big step ahead could be to use reinforcement learning for power system stability surveillance which can train the deep learning models online simultaneously with the present data while also monitoring the system at the same time. The utilization of artificial intelligence for online training and online applications of the monitoring system could be a huge step in this direction.

Bibliography

[1] A. Hoballah, *Power System Stability Assessment and Enhancement using Computational Intelligence*. PhD thesis, 2011.

[2] P. Kundur, J. Paserba, V. Ajjarapu, G. Andersson, A. Bose, C. Canizares, N. Hatziargyriou, D. Hill, A. Stankovic, C. Taylor, T. Van Cutsem, and V. Vittal, "Definition and classification of power system stability ieee/cigre joint task force on stability terms and definitions," *IEEE Transactions on Power Systems*, vol. 19, pp. 1387–1401, Aug 2004.

[3] M. J. Basler and R. C. Schaefer, "Understanding power system stability," in *58th IEEE Annual Conference for Protective Relay Engineers, 2005.*, pp. 46–67, 2005.

[4] V. Vittal and A. Bergen, "Power systems analysis," *Prentice Hall*, pp. 1–2, 1999.

[5] M. Jha, S. Chakrabarti, and E. Kyriakides, "Estimation of the rotor angle of a synchronous generator by using PMU measurements," in *2015 IEEE Eindhoven PowerTech*, pp. 1–6, June 2015.

[6] G. Andersson, P. Donalek, R. Farmer, N. Hatziargyriou, I. Kamwa, P. Kundur, N. Martins, J. Paserba, P. Pourbeik, J. Sanchez-Gasca, *et al.*, "Causes of the 2003 major grid blackouts in north america and europe, and recommended means to improve system dynamic performance," *IEEE Transactions on Power Systems*, vol. 20, no. 4, pp. 1922–1928, 2005.

[7] L. L. Lai, *Power system restructuring and deregulation: trading, performance and information technology*. John Wiley & Sons, 2001.

[8] N. A. E. R. C. (NERC), "2009 long-term reliability assessment." `https://www.nerc.com/pa/RAPA/ra/Reliability%20Assessments%20DL/2009_LTRA_v1_1_errata.pdf`, October 2009.

[9] P. Dehghanian, Y. Guan, and M. Kezunovic, "Real-time life-cycle assessment of high voltage circuit breakers for maintenance using online condition monitoring data," *IEEE Transactions on Industry Applications*, vol. 55, no. 2, pp. 1135–1146, 2019.

[10] P. Dehghanian and M. Kezunovic, "Probabilistic decision making for the bulk power system optimal topology control," *IEEE Transactions on Smart Grid*, vol. 7, no. 4, pp. 2071–2081, 2016.

[11] P. Dehghanian, Y. Wang, G. Gurrala, E. Moreno-Centeno, and P. Kezunovic, "Flexible implementation of power system corrective topology control," *Electric Power System Research*, vol. 128, pp. 79–89, 2015.

[12] M. Alhazmi, P. Dehghanian, S. Wang, and B. Shinde, "Power grid optimal topology control considering correlations of system uncertainties," in *IEEE/IAS 55th Industrial and Commercial Power Systems (I&CPS) Technical Conference*, pp. 1–7, 2019.

[13] M. Kezunovic, T. Popovic, G. Gurrala, P. Dehghanian, A. Esmaeilian, and M. Tasdighi, "Reliable implementation of robust adaptive topology control," in *The 47th Hawaii International Conference on System Science (HICSS)*, pp. 1–10, 2014.

[14] P. Dehghanian and M. Kezunovic, "Impact assessment of power system topology control on system reliability," in *IEEE Conference on Intelligent Systems Applications to Power Systems (ISAP)*, pp. 1–6, 2015.

[15] P. Dehghanian and M. Kezunovic, "Probabilistic impact of transmission line switching on power system operating states," in *IEEE Power and Energy Society (PES) Transmission and Distribution (T&D) Conference and Exposition*, pp. 1–6, 2016.

[16] M. Alhazmi, P. Dehghanian, S. Wang, and B. Shinde, "Power grid optimal topology control considering correlations of system uncertainties," *IEEE Transactions on Industry Applications*, vol. 55, no. 6, pp. 5594–5604, 2019.

[17] M. A. Saffari, M. S. Misaghian, M. Kia, Heidari, and P. Dehghanian, "Robust/stochastic optimization of energy arbitrage in smart microgrids using electric vehicles," *Electric Power Systems Research*, vol. 174, pp. 1–14, 2019.

[18] M. Moeini-Aghtaie, A. Abbaspour, M. Fotuhi-Firuzabad, and P. Dehghanian, "Optimized probabilistic phev demand management in the context of energy hubs," *IEEE Transactions on Power Delivery*, vol. 30, no. 2, pp. 996–1006, 2015.

[19] M. Moeini-Aghtaie, P. Dehghanian, M. Fotuhi-Firuzabad, and A. Abbaspour, "Multiagent genetic algorithm: An online probabilistic view on economic dispatch of energy hubs constrained by wind availability," *IEEE Transactions on Sustainable Energy*, vol. 5, no. 2, pp. 699–708, 2014.

[20] P. Dehghanian, S. H. Hosseini, M. Moeini-Aghtaie, and S. Arabali, "Optimal siting of dg units in power systems from a probabilistic multi-objective optimization perspective," *International Journal of Electrical Power and Energy Systems*, vol. 51, pp. 14–26, 2013.

[21] M. Moeini-Aghtaie, A. Abbaspour, M. Fotuhi-Firuzabad, and P. Dehghanian, "Phev's centralized/decentralized charging control mechanisms: Requirements and impacts," in *The 45th North American Power Symposium (NAPS)*, pp. 1–6, 2013.

[22] M. S. Misaghian, M. Saffari, M. Kia, A. Heidari, P. Dehghanian, and B. Wang, "Electric vehicles contributions to voltage improvement and loss reduction in microgrids," in *North American Power Symposium (NAPS)*, pp. 1–6, 2018.

[23] B. Wang, P. Dehghanian, S. Wang, and M. Mitolo, "Electrical safety considerations in large electric vehicle charging stations," *IEEE Transactions on Industry Applications*, vol. 55, no. 6, pp. 6603–6612, 2019.

[24] B. Wang, P. Dehghanian, and D. Zhao, "Chance-constrained energy management system for power grids with high proliferation of renewables and electric vehicles," *IEEE Transactions on Smart Grid*, pp. 1–13, 2019.

[25] A. Razi-Kazemi and P. Dehghanian, "A practical approach to optimal RTU placement in power distribution systems incorporating fuzzy sets theory," *International Journal of Electrical Power and Energy Systems*, vol. 37, no. 1, pp. 31–42, 2012.

[26] P. Dehghanian, A. Razi-Kazemi, and M. Fotuhi-Firuzabad, "Optimal RTU placement in power distribution systems using a novel method based on analytical hierarchical process (AHP)," in *The 10th International IEEE Conference on Environmental and Electrical Engineering (EEEIC)*, pp. 1–6, 2011.

[27] M. Moeini-Aghtaie, P. Dehghanian, and S. H. Hosseini, "Optimal distributed generation placement in a restructured environment via a multi-objective optimization approach," in *16th Conference on Electric Power Distribution Networks (EPDC)*, pp. 1–6, 2011.

[28] A. Razi-Kazemi, P. Dehghanian, and G. Karami, "A probabilistic approach for remote terminal unit placement in power distribution systems," in *The 33rd IEEE International Telecommunications Energy Conference (INTELEC)*, pp. 1–6, 2011.

[29] P. Dehghanian, A. Razi-Kazemi, and G. Karami, "Incorporating experts knowledge in RTU placement procedure using fuzzy sets theory- a practical approach," in *The 33rd IEEE International Telecommunications Energy Conference (INTELEC)*, pp. 1–6, 2011.

[30] M. Shojaei, V. Rastegar-Moghaddam, A. Razi-Kazemi, P. Dehghanian, and G. Karami, "A new look on the automation of medium voltage substations in power distribution systems," in *17th Conference on Electric Power Distribution Networks (EPDC)*, pp. 1–6, 2012.

[31] T. Becejac and P. Dehghanian, "PMU multilevel end-to-end testing to assess synchrophasor measurements during faults," *IEEE Power and Energy Technology Systems Journal*, vol. 6, no. 1, pp. 71–80, 2019.

[32] S. Wang, P. Dehghanian, and B. Zhang, "A data-driven algorithm for online power grid topology change identification with PMUs," in *IEEE Power and Energy Society (PES) General Meeting*, pp. 1–5, 2019.

[33] S. Wang, P. Dehghanian, and Y. Gu, "A novel multi-resolution wavelet transform for online power grid waveform classification," in *The 1st IEEE International Conference on Smart Grid Synchronized Measurements and Analytics (SGSMA)*, pp. 1–6, 2019.

[34] M. Kezunovic, A. Esmaeilian, T. Becejac, P. Dehghanian, and C. Qian, "Life-cycle management tools for synchrophasor systems: Why we need them and what they should entail," in *The 2016 IFAC CIGRE/CIRED Workshop on Control of Transmission and Distribution Smart Grids*, pp. 1–6, CIGRE, 2016.

[35] T. Becejac, P. Dehghanian, and M. Kezunovic, "Analysis of PMU algorithm errors during fault transients and out-of-step disturbances," in *IEEE Power and Energy Society (PES) Transmission & Distribution (T&D) Conference and Exposition Latin America*, pp. 1–6, 2016.

[36] T. Becejac, P. Dehghanian, and M. Kezunovic, "Probabilistic assessment of PMU integrity for planning of periodic maintenance and testing," in *International Conference on Probabilistic Methods Applied to Power Systems (PMAPS)*, pp. 1–6, 2016.

[37] T. Becejac, P. Dehghanian, and M. Kezunovic, "Impact of PMU errors on the synchrophasor-based fault location algorithms," in *48th North American Power Symposium (NAPS)*, pp. 1–6, 2016.

[38] M. Kezunovic, P. Dehghanian, and J. Sztipanovits, "An incremental system-of-systems integration modelling of cyber-physical electric power systems," in *Grid of the Future Symposium, CIGRE US National Committee*, pp. 1–6, CIGRE, 2016.

[39] M. H. Rezaeian Koochi, P. Dehghanian, S. Esmaeili, P. Dehghanian, and S. Wang, "A synchrophasor-based decision tree approach for identification of most coherent generating units," in *The 44th Annual Conference of the IEEE Industrial Electronics Society (IECON)*, pp. 1–6, 2018.

[40] Z. Tayebi and B. Najafi, "Determination of vulnerability and risk management in microcredit programs: applying risk sharing model and panel data approach," *Iranian Journal of Agricultural Economics*, vol. 5, no. 4, pp. 25–49, 2012.

[41] Z. Tayebi and L. E. Fulginiti, "Agricultural productivity and climate change in the greater middle east," 2016.

[42] Z. Tayebi and G. Onel, "Revisiting the neoclassical model of out-farm migration: Evidence from nonlinear panel time series data," *Agricultural and Applied Economics Association Annual Meeting*, 2017.

[43] B. Zhang, P. Dehghanian, and M. Kezunovic, "Simulation of weather impacts on the wholesale electricity market," in *10th International Conference on Deregulated Electricity Market Issues in South Eastern Europe (DEMSEE)*, pp. 1–6, 2015.

[44] T. Dokic, P. Dehghanian, P.-C. Chen, M. Kezunovic, Z. Medina-Cetina, J. Stojanovic, and Z. Obradovic, "Risk assessment of a transmission line insulation breakdown due to lightning and severe weather," in *The 49th Hawaii International Conference on System Science (HICSS)*, pp. 1–8, 2016.

[45] B. Zhang, P. Dehghanian, and M. Kezunovic, "Spatial-temporal solar power forecast through gaussian conditional random fields," in *IEEE Power and Energy Society (PES) General Meeting*, pp. 1–5, 2016.

[46] P. Dehghanian, S. Aslan, and P. Dehghanian, "Quantifying power system resiliency improvement using network reconfiguration," in *IEEE 60th International Midwest Symposium on Circuits and Systems (MWSCAS)*, pp. 1–5, 2017.

[47] P. Dehghanian, B. Zhang, T. Dokic, and M. Kezunovic, "Predictive risk analytics for weather-resilient operation of electric power systems," *IEEE Transactions on Sustainable Energy*, vol. 10, no. 1, pp. 3–15, 2019.

[48] P. Dehghanian, S. Aslan, and P. Dehghanian, "Maintaining electric system safety through an enhanced network resilience," *IEEE Transactions on Industry Applications*, vol. 54, no. 5, pp. 4927–4937, 2018.

[49] B. Zhang, P. Dehghanian, and M. Kezunovic, "Optimal allocation of PV generation and battery storage for enhanced resilience," *IEEE Transactions on Smart Grid*, vol. 10, no. 1, pp. 535–545, 2017.

[50] M. Nazemi, M. Moeini-Aghtaie, M. Fotuhi-Firuzabad, and P. Dehghanian, "Energy storage planning for enhanced resilience of power distribution networks against earthquakes," *IEEE Transactions on Sustainable Energy*, pp. 1–1, 2019.

[51] J. Lai, X. Lu, F. Wang, P. Dehghanian, and R. Tang, "Broadcast gossip algorithms for distributed peer-to-peer control in AC microgrids," *IEEE Transactions on Industry Applications*, vol. 55, no. 3, pp. 2241–2251, 2019.

[52] S. Wang, P. Dehghanian, M. Alhazmi, J. Su, and B. Shinde, "Resilience-assured protective control of DC/AC inverters under unbalanced and fault scenarios," in *The 10th IEEE Power and Energy Society (PES) Conference on Innovative Smart Grid Technologies-North America (ISGT-NA)*, pp. 1–5, 2019.

[53] S. Wang, P. Dehghanian, and Y. Gu, "A novel multi-resolution wavelet transform for online power grid waveform classification," in *The 1st IEEE International Conference on Smart Grid Synchronized Measurements and Analytics (SGSMA)*, pp. 1–6, 2019.

[54] S. Wang, P. Dehghanian, and B. Zhang, "A data-driven algorithm for online power grid topology change identification with PMUs," in *IEEE Power and Energy Society (PES) General Meeting*, pp. 1–5, 2019.

[55] R. Araneo, P. Dehghanian, and M. Mitolo, "Electrical safety of academic laboratories," in *IEEE/IAS 55th Industrial and Commercial Power Systems (ICPS) Technical Conference*, pp. 1–6, 2019.

[56] S. Wang, L. Li, and P. Dehghanian, "Power grid online surveillance through PMU-embedded convolutional neural networks," in *IEEE Industry Applications Society (IAS) Annual Meeting*, pp. 1–7, 2019.

[57] M. Nazemi, P. Dehghanian, and M. Lejeune, "A mixed-integer distributionally robust chance-constrained model for optimal topology control in power grids with uncertain renewables," in *13th IEEE Power and Energy Society (PES) PowerTech Conference*, pp. 1–6, 2019.

[58] F. Wang, B. Xiang, K. Li, J. Lai, and P. Dehghanian, "Day-ahead forecast of aggregated loads for smart households under incentive-based demand response programs," in *IEEE Industry Applications Society (IAS) Annual Meeting*, pp. 1–10, 2019.

[59] Z. Yang, P. Dehghanian, and M. Nazemi, "Enhancing seismic resilience of electric power distribution systems with mobile power sources," in *IEEE Industry Applications Society (IAS) Annual Meeting*, pp. 1–7, 2019.

[60] S. Wang, P. Dehghanian, L. Li, and B. Wang, "A machine learning approach to detection of geomagnetically-induced currents in power grids," in *IEEE Industry Applications Society (IAS) Annual Meeting*, pp. 1–7, 2019.

[61] J. Su, P. Dehghanian, M. Nazemi, and B. Wang, "Distributed wind power resources for enhanced power grid resilience," in *The 51st North American Power Symposium (NAPS)*, pp. 1–6, 2019.

[62] D. Wang, Y. Li, P. Dehghanian, and S. Wang, "Power grid resilience to electromagnetic (EMP) disturbances: A literature review," in *The 51st North American Power Symposium (NAPS)*, pp. 1–6, 2019.

[63] S. Wang, P. Dehghanian, and L. Li, "PMU2.0: A smart sensor solution for online situational awareness in power grids," in *XXI Power Systems Computation Conference (PSCC)*, pp. 1–6, 2020.

[64] Z. Yang, M. Nazemi, P. Dehghanian, and M. Barati, "Toward resilient solar-integrated distribution grids: Harnessing the mobility of power sources," in *IEEE Power and Energy Society (PES) Transmission and Distribution (TD) Conference and Exposition*, pp. 1–5, 2020.

[65] B. Shinde, S. Wang, P. Dehghanian, and M. Babakmehr, "Real-time detection of critical generators in power systems: A deep learning HCP approach," in *The 4th IEEE Texas Power and Energy Conference (TPEC)*, pp. 1–6, 2020.

[66] S. Wang, P. Dehghanian, M. Alhazmi, and M. Nazemi, "Advanced control solutions for enhanced resilience of modern power-electronic-interfaced distribution systems," *Journal of Modern Power Systems and Clean Energy*, vol. 7, no. 4, pp. 716–730, 2019.

[67] M. Khoshjahan, P. Dehghanian, M. Moeini-Aghtaie, and M. Fotuhi-Firuzabad, "Harnessing ramp capability of spinning reserve services for enhanced power system flexibility," *IEEE Transactions on Industry Applications*, vol. 55, no. 6, pp. 7103–7112, 2019.

[68] R. Araneo, P. Dehghanian, and M. Mitolo, "On electrical safety in academic laboratories," *IEEE Transactions on Industry Applications*, vol. 55, no. 6, pp. 5613–5620, 2019.

[69] F. Pourahmadi, H. Heidarabadi, S. Hosseini, and P. Dehghanian, "Dynamic uncertainty set characterization for bulk power grid flexibility assessment," *IEEE Systems Journal*, pp. 1–11, 2019.

[70] P. Jamborsalamati, M. Hossain, S. Taghizadeh, A. Sadu, G. Konstantinou, M. Manbachi, and P. Dehghanian, "Enhancing power grid resilience through an IEC61850-based ev-assisted load restoration," *IEEE Transactions on Industrial Informatics*, pp. 1–11, 2019.

[71] H. Tarzamni, E. Babaei, F. Panahandeh Esmaeelnia, P. Dehghanian, S. Tohidi, and M. Bannae Sharifian, "Analysis and reliability evaluation of a high step-up soft switching push-pull DC-DC converter," *IEEE Transactions on Reliability*, pp. 1–11, 2019.

[72] H. Tarzamni, F. Panahandeh Esmaeelnia, M. Fotuhi-Firuzabad, F. Tahami, S. Tohidi, and P. Dehghanian, "Comprehensive analytics for reliability evaluation of conventional isolated multi-switch PWM DC-DC converters," *IEEE Transactions on Power Electronics*, pp. 1–13, 2019.

[73] M. Nazemi and P. Dehghanian, "Seismic-resilient bulk power grids: Hazard characterization, modeling, and mitigation," *IEEE Transactions on Engineering Management*, pp. 1–17, 2019.

[74] M. Zareian Jahromi, M. Tajdinian, J. Zhao, P. Dehghanian, M. Allahbakhshi, and A. Seifi, "An enhanced sensitivity-based decentralized framework for real-time transient stability assessment in bulk power grids with renewable energy resources," *IET Generation, Transmission, and Distribution Systems*, pp. 1–10, 2019.

[75] S. Wang, P. Dehghanian, L. Li, and B. Wang, "A machine learning approach to detection of geomagnetically-induced currents in power grids," *IEEE Transactions on Industry Applications*, pp. 1–9, 2019.

[76] S. Wang, P. Dehghanian, and L. Li, "Power grid online surveillance through PMU-embedded convolutional neural networks," *IEEE Transactions on Industry Applications*, pp. 1–10, 2019.

[77] F. Pourahmadi, H. Heidarabadi, S. H. Hosseini, and P. Dehghanian, "Dynamic uncertainty set characterization for bulk power grid flexibility assessment," *IEEE Systems Journal*, 2019.

[78] R. Azizpanah-Abarghooee, P. Dehghanian, and V. Terzija, "A practical multi-area bi-objective environmental economic dispatch equipped with a hybrid gradient search method and improved jaya algorithm," *IET Generation, Transmission & Distribution*, vol. 10, no. 14, pp. 3580–3596, 2016.

[79] F. Pourahmadi and P. Dehghanian, "A game-theoretic loss allocation approach in power distribution systems with high penetration of distributed generations," *Mathematics*, vol. 6, no. 9, pp. 1–14, 2018.

[80] P. Dehghanian, M. Fotuhi-Firuzabad, F. Aminifar, and R. Billinton, "A comprehensive scheme for reliability centered maintenance implementation in power distribution systems- part II: Numerical analysis," *IEEE Transactions on Power Delivery*, vol. 28, no. 2, pp. 771–778, 2013.

[81] S. Moradi, V. vahidinasab, M. Kia, and P. Dehghanian, "A mathematical framework for reliability-centered asset management implementation in microgrids," *International Transactions on Electrical Energy Systems*, 2018.

[82] H. Mirsaeedi, A. Fereidunian, S. M. Mohammadi-Hosseininejad, P. Dehghanian, and H. Lesani, "Long-term maintenance scheduling and budgeting in electricity distribution systems equipped with automatic switches," *IEEE Transactions on Industrial Informatics*, vol. 14, no. 5, pp. 1909–1919, 2018.

[83] M. Asghari Gharakheili, M. Fotuhi-Firuzabad, and P. Dehghanian, "A new multi-attribute support tool for identifying critical components in power transmission systems," *IEEE Systems Journal*, vol. 12, no. 1, pp. 316–327, 2018.

[84] F. Pourahmadi, M. Fotuhi-Firuzabad, and P. Dehghanian, "Application of game theory in reliability centered maintenance of electric power systems," *IEEE Transactions on Industry Applications*, vol. 53, no. 2, pp. 936–946, 2017.

[85] F. Pourahmadi, M. Fotuhi-Firuzabad, and P. Dehghanian, "Identification of critical generating units for maintenance: A game theory approach," *IET Generation, Transmission & Distribution*, vol. 10, no. 12, pp. 2942–2952, 2016.

[86] H. Sabouhi, A. Abbaspour, M. Fotuhi-Firuzabad, and P. Dehghanian, "Identifying critical components of combined cycle power plants for implementation of reliability centered maintenance," *IEEE CSEE Journal of Power and Energy Systems*, vol. 2, no. 2, pp. 87–97, 2016.

[87] H. Sabouhi, A. Abbaspour, M. Fotuhi-Firuzabad, and P. Dehghanian, "Reliability modeling and availability analysis of combined cycle power plants," *International Journal of Electrical Power and Energy Systems*, vol. 79, pp. 108–119, 2016.

[88] R. Ghorani, M. Fotuhi-Firuzabad, P. Dehghanian, and W. Li, "Identifying critical component for reliability centered maintenance management of deregulated power systems," *IET Generation, Transmission, and Distribution*, vol. 9, no. 9, pp. 828–837, 2015.

[89] P. Dehghanian, M. Fotuhi-Firuzabad, S. Bagheri-Shoraki, and A. Razi-Kazemi, "Critical component identification in reliability centered asset management of distribution power systems via fuzzy ahp," *IEEE Systems Journal*, vol. 6, no. 4, pp. 593–602, 2012.

[90] P. Dehghanian, M. Fotuhi-Firuzabad, F. Aminifar, and R. Billinton, "A comprehensive scheme for reliability centered maintenance implementation in power distribution systems- part I: Methodology," *IEEE Transactions on Power Delivery*, vol. 28, no. 2, pp. 761–770, 2013.

[91] P. Dehghanian, M. Fotuhi-Firuzabad, and A. Razi-Kazemi, "An approach for critical component identification in reliability-centered maintenance of power distribution systems based on analytical hierarchical process," in *The 21st International Conference and Exhibition on Electricity Distribution (CIRED)*, pp. 1–4, 2011.

[92] P. Dehghanian and M. Fotuhi-Firuzabad, "A reliability-oriented outlook on the critical components of power distribution systems," in *The 9th IET International Conference on Advances in Power System Control, Operation, and Management (APSCOM)*, pp. 1–6, 2011.

[93] P. Dehghanian, M. Kezunovic, G. Gurrala, and Y. Guan, "Security-based circuit breaker maintenance management," in *IEEE Power and Energy Society (PES) General Meeting*, pp. 1–5, 2013.

[94] K. M. Guan, Yufan, P. Dehghanian, and G. Gurrala, "Assessing circuit breaker life cycle using condition-based data," in *IEEE Power and Energy Society (PES) General Meeting*, pp. 1–5, 2013.

[95] P. Dehghanian, Y. Guan, and M. Kezunovic, "Real-time life-cycle assessment of circuit breakers for maintenance using online condition monitoring data," in *IEEE/IAS 54th Industrial and Commercial Power Systems (I&CPS) Technical Conference*, pp. 1–8, 2018.

[96] F. Pourahmadi, M. Fotuhi-Firuzabad, and P. Dehghanian, "Identification of critical components in power systems: A game theory application," in *IEEE Industry Application Society (IAS) Annual Meeting*, pp. 1–6, 2016.

[97] P. Dehghanian, T. Popovic, and M. Kezunovic, "Circuit breaker operational health assessment via condition monitoring data," in *The 46th North American Power Symposium*, pp. 1–6, 2014.

[98] P. Dehghanian, M. Moeini-Aghtaie, M. Fotuhi-Firuzabad, and R. Billinton, "A practical application of the delphi method in maintenance-targeted resource allocation of distribution utilities," in *The 13th International Conference on Probabilistic Methods Applied to Power Systems (PMAPS)*, pp. 1–6, 2014.

[99] P. Dehghanian and M. Kezunovic, "Cost/benefit analysis for circuit breaker maintenance planning and scheduling," in *The 45th North American Power Symposium (NAPS)*, pp. 1–6, 2013.

[100] C. P. Steinmetz, "Power control and stability of electric generating stations," *Transactions of the American Institute of Electrical Engineers*, vol. 39, no. 2, pp. 1215–1287, 1920.

[101] "First report of power system stability," *Transactions of the American Institute of Electrical Engineers*, vol. 56, pp. 261–282, Feb 1937.

[102] G. S. Vassell, "Northeast blackout of 1965," *IEEE Power Engineering Review*, vol. 11, pp. 4–, January 1991.

[103] M. EL-Shimy, "This is how you cite a website in latex." `https://www.researchgate.net/publication/323073706_POWER_SYSTEM_STABILITY_-_A_technical_report_and_a_short_course`, February 2018.

[104] P. Kundur, N. J. Balu, and M. G. Lauby, *Power system stability and control*, vol. 7. McGraw-hill New York, 1994.

[105] V. I. Vorotnikov, *Partial stability and control*. Springer Science & Business Media, 2012.

[106] N. Rouche, P. Habets, and M. Laloy, *Stability theory by Liapunov's direct method*, vol. 4. Springer, 1977.

[107] C. T. F. . Rep, "Analysis and modeling needs of power systems under major frequency disturbances." `http://precog.iiitd.edu.in/people/anupama`, January 1999.

[108] P. Kundur, D. C. Lee, J. P. Bayne, and P. L. Dandeno, "Impact of turbine generator overspeed controls on unit performance under system disturbance conditions," *IEEE Power Engineering Review*, vol. PER-5, pp. 28–29, June 1985.

[109] H. H. Al Marhoon, "Adaptive online transient stability assessment of power systems for operational purposes," 2015.

[110] V. Lackovic, "Power system transient stability study fundamentals." `https://www.cedengineering.com/userfiles/Power%20System%20Transient%20Stability%20Study%20Fundamentals.pdf`.

[111] P. K. Iyambo and R. Tzoneva, "Transient stability analysis of the ieee 14-bus electric power system," in *AFRICON 2007*, pp. 1–9, Sep. 2007.

[112] J. S. Patel and M. N. Sinha, "Power system transient stability analysis using etap software," in *National Conference on Recent Trends in Engineering & Technology*, pp. 13–14, 2011.

[113] K. Mishra and S. Umredkar, "Transient stability analysis of multi machine system," *International Journal of Science and Research IJSR*, vol. 2, no. 4, 2013.

[114] K. S. Shetye, T. J. Overbye, and J. F. Gronquist, "Validation of power system transient stability results," in *2012 IEEE Power and Energy Conference at Illinois*, pp. 1–8, Feb 2012.

[115] B. Tan, J. Yang, X. Pan, J. Li, P. Xie, and C. Zeng, "Representational learning approach for power system transient stability assessment based on convolutional neural network," *The Journal of Engineering*, vol. 2017, no. 13, pp. 1847–1850, 2017.

[116] A. Hoballah and I. Erlich, "Transient stability assessment using ann considering power system topology changes," in *2009 15th International Conference on Intelligent System Applications to Power Systems*, pp. 1–6, 2009.

[117] M. Pavella, D. Ernst, and D. Ruiz-Vega, *Transient stability of power systems: a unified approach to assessment and control*. Springer Science & Business Media, 2012.

[118] S. Wei, M. Yang, J. Qi, J. Wang, S. Ma, and X. Han, "Model-free mle estimation for online rotor angle stability assessment with PMU data," *IEEE Transactions on Power Systems*, vol. 33, pp. 2463–2476, May 2018.

[119] Z. Huang, K. Schneider, and J. Nieplocha, "Feasibility studies of applying kalman filter techniques to power system dynamic state estimation," in *2007 IEEE International Power Engineering Conference (IPEC 2007)*, pp. 376–382, 2007.

[120] E. Ghahremani and I. Kamwa, "Dynamic state estimation in power system by applying the extended kalman filter with unknown inputs to phasor measurements," *IEEE Transactions on Power Systems*, vol. 26, pp. 2556–2566, Nov 2011.

[121] K. Sun, J. Qi, and W. Kang, "Power system observability and dynamic state estimation for stability monitoring using synchrophasor measurements," *Control Engineering Practice*, vol. 53, pp. 160–172, 2016.

[122] E. Ghahremani and I. Kamwa, "Local and wide-area PMU-based decentralized dynamic state estimation in multi-machine power systems," *IEEE Transactions on Power Systems*, vol. 31, pp. 547–562, Jan 2016.

[123] J. Qi, K. Sun, J. Wang, and H. Liu, "Dynamic state estimation for multi-machine power system by unscented kalman filter with enhanced numerical stability," *IEEE Transactions on Smart Grid*, vol. 9, pp. 1184–1196, March 2018.

[124] K. Padiyar, *Power system dynamics: stability and control*. John Wiley New York, 1996.

[125] P. Kundur, "Power system stability and control. mcgrawhill, london, 1994. pikeresearch. worldwide revenue from microgridswill reach $17.3 billion by 2017," tech. rep., Technical report, Pike Research, 2012. URL http://www. pikeresearch. com ....

[126] M. Pai, *Energy function analysis for power system stability*. Springer Science & Business Media, 2012.

[127] S. E. Stanton, "Transient stability monitoring for electric power systems using a partial energy function," *IEEE Transactions on Power Systems*, vol. 4, pp. 1389–1396, Nov 1989.

[128] Y. Xue, T. Van Custem, and M. Ribbens-Pavella, "Extended equal area criterion justifications, generalizations, applications," *IEEE Transactions on Power Systems*, vol. 4, pp. 44–52, Feb 1989.

[129] D. Ruiz-Vega and M. Pavella, "A comprehensive approach to transient stability control. i. near optimal preventive control," *IEEE Transactions on Power Systems*, vol. 18, pp. 1446–1453, Nov 2003.

[130] C. A. Jensen, M. A. El-Sharkawi, and R. J. Marks, "Power system security assessment using neural networks: feature selection using fisher discrimination," *IEEE Transactions on Power Systems*, vol. 16, pp. 757–763, Nov 2001.

[131] L. S. Moulin, A. P. A. da Silva, M. A. El-Sharkawi, and R. J. Marks, "Support vector machines for transient stability analysis of large-scale power systems," *IEEE Transactions on Power Systems*, vol. 19, pp. 818–825, May 2004.

[132] A. Gavoyiannis, D. Vogiatzis, D. Georgiadis, and N. Hatziargyriou, "Combined support vector classifiers using fuzzy clustering for dynamic security assessment," in *2001 Power Engineering Society Summer Meeting. Conference Proceedings (Cat. No. 01CH37262)*, vol. 2, pp. 1281–1286, 2001.

[133] K. Chen, J. Hu, and J. He, "Detection and classification of transmission line faults based on unsupervised feature learning and convolutional sparse autoencoder," in *2017 IEEE Power Energy Society General Meeting*, pp. 1–1, July 2017.

[134] C. Zheng, V. Malbasa, and M. Kezunovic, "Regression tree for stability margin prediction using synchrophasor measurements," *IEEE Transactions on Power Systems*, vol. 28, pp. 1978–1987, May 2013.

[135] L. Wehenkel, T. Van Cutsem, and M. Ribbens-Pavella, "An artificial intelligence framework for online transient stability assessment of power systems," *IEEE Transactions on Power Systems*, vol. 4, no. 2, pp. 789–800, 1989.

[136] L. Wehenkel, M. Pavella, E. Euxibie, and B. Heilbronn, "Decision tree based transient stability method a case study," *IEEE Transactions on Power Systems*, vol. 9, pp. 459–469, Feb 1994.

[137] F. R. Gomez, A. D. Rajapakse, U. D. Annakkage, and I. T. Fernando, "Support vector machine-based algorithm for post-fault transient stability status prediction using synchronized measurements," *IEEE Transactions on Power Systems*, vol. 26, pp. 1474–1483, Aug 2011.

[138] A. Rajapakse, F. Gomez, K. Nanayakkara, P. Crossley, and V. Terzija, "Rotor angle instability prediction using post-disturbance voltage trajectories," in *IEEE Power and Energy Society General Meeting*, pp. 1–1, July 2010.

[139] J. J. Q. Yu, D. J. Hill, A. Y. S. Lam, J. Gu, and V. O. K. Li, "Intelligent time-adaptive transient stability assessment system," *IEEE Transactions on Power Systems*, vol. 33, pp. 1049–1058, Jan 2018.

[140] H. Al Marhoon, I. Leevongwat, and P. Rastgoufard, "A practical method for power systems transient stability and security analysis," in *IEEE Power and Energy Society Transmission & Distribution Conference and Exposition*, pp. 1–6, 2012.

[141] M. Pavella, D. Ernst, and D. Ruiz-Vega, *Transient stability of power systems: a unified approach to assessment and control*. Springer Science & Business Media, 2012.

[142] A. Hoballah and I. Erlich, "Generation coordination for transient stability enhancement using particle swarm optimization," in *12th IEEE International Middle-East Power System Conference*, pp. 29–33, 2008.

[143] A. Gupta, G. Gurrala, and P. S. Sastry, "An online power system stability monitoring system using convolutional neural networks," *IEEE Transactions on Power Systems*, vol. 34, pp. 864–872, March 2019.

[144] Y. Wei, W. Xia, M. Lin, J. Huang, B. Ni, J. Dong, Y. Zhao, and S. Yan, "Hcp: A flexible cnn framework for multi-label image classification," *IEEE Transactions on Pattern Analysis and Machine Intelligence*, vol. 38, pp. 1901–1907, Sep. 2016.

[145] E. W. Kimbark, *Power system stability*, vol. 1. John Wiley & Sons, 1995.

[146] P. M. Anderson and A. A. Fouad, *Power system control and stability*. John Wiley & Sons, 2008.

[147] V. Venkatasubramanian and R. G. Kavasseri, "Direct computation of generator internal dynamic states from terminal measurements," in *Proceedings of the 37th IEEE Annual Hawaii International Conference on System Sciences (HICSS)*, pp. 6–pp, IEEE, 2004.

[148] E. Ghahremani, M. Karrari, and O. Malik, "Synchronous generator third-order model parameter estimation using online experimental data," *IET generation, transmission & distribution*, vol. 2, no. 5, pp. 708–719, 2008.

[149] Y. LeCun, Y. Bengio, *et al.*, "Convolutional networks for images, speech, and time series," *The Handbook of Brain Theory and Neural Networks*, vol. 3361, no. 10, p. 1995, 1995.

[150] Y. A. LeCun, L. Bottou, G. B. Orr, and K.-R. M*ü*ller, "Efficient backprop," in *Neural Networks: Tricks of the Trade*, pp. 9–48, Springer, 2012.

[151] A. Xavier, "An introduction to convlstm." https://medium.com/neuronio/an-introduction-to-convlstm-55c9025563a7, March.

[152] S. Xingjian, Z. Chen, H. Wang, D.-Y. Yeung, W.-K. Wong, and W.-c. Woo, "Convolutional lstm network: A machine learning approach for precipitation nowcasting," in *Advances in Neural Information Processing Systems (NIPS)*, pp. 802–810, 2015.

[153] A. Graves, "Generating sequences with recurrent neural networks," *arXiv preprint arXiv:1308.0850*, 2013.

[154] S. Hochreiter and J. Schmidhuber, "Long short-term memory," *Neural Computation*, vol. 9, no. 8, pp. 1735–1780, 1997.

[155] R. Pascanu, T. Mikolov, and Y. Bengio, "On the difficulty of training recurrent neural networks," in *International Conference on Machine Learning*, pp. 1310–1318, 2013.

[156] I. Sutskever, O. Vinyals, and Q. Le, "Sequence to sequence learning with neural networks," *Neural Information Processing Systems (NIPS)*, 2014.

[157] S. A. Rahman and D. A. Adjeroh, "Deep learning using convolutional lstm estimates biological age from physical activity," *Scientific Reports*, vol. 9, no. 1, pp. 1–15, 2019.

[158] S. Kim, S. Hong, M. Joh, and S.-k. Song, "Deeprain: Convlstm network for precipitation prediction using multichannel radar data," *arXiv preprint arXiv:1711.02316*, 2017.

[159] W.-S. Hu, H.-C. Li, L. Pan, W. Li, R. Tao, and Q. Du, "Feature extraction and classification based on spatial-spectral convlstm neural network for hyperspectral images," *arXiv preprint arXiv:1905.03577*, 2019.

[160] A. Budhiraja, "Dropout in (deep) machine learning." `https://medium.com/@amarbudhiraja/`, December 2016.

[161] R. Wan, S. Mei, J. Wang, M. Liu, and F. Yang, "Multivariate temporal convolutional network: A deep neural networks approach for multivariate time series forecasting," *Electronics*, vol. 8, no. 8, p. 876, 2019.

[162] A. R. Al-Roomi, "Power Flow Test Systems Repository," 2015.

Appendix 1: Case Study I Data for the IEEE 118-Bus Test System

In case study I, the implementation of the CNN-HCP NN model is pursued on the IEEE 118-bus test system shown in Figure 1 [162]. The information regarding the case summary of the specified model is shown in Table 1 and 2. The transient stability analysis simulations are run in PowerWorld software environment for faults at each bus and transmission line. The machine models, exciter, governor and stabilizer of the generators and other general information are provided in Table 3. The values of model parameters used for modeling the generator machines is shown in Table 4 and 5. The table includes generator information for 19 generators with real power data only. Along with information regarding generation of power system, loading information at the base case is given in Table 6.

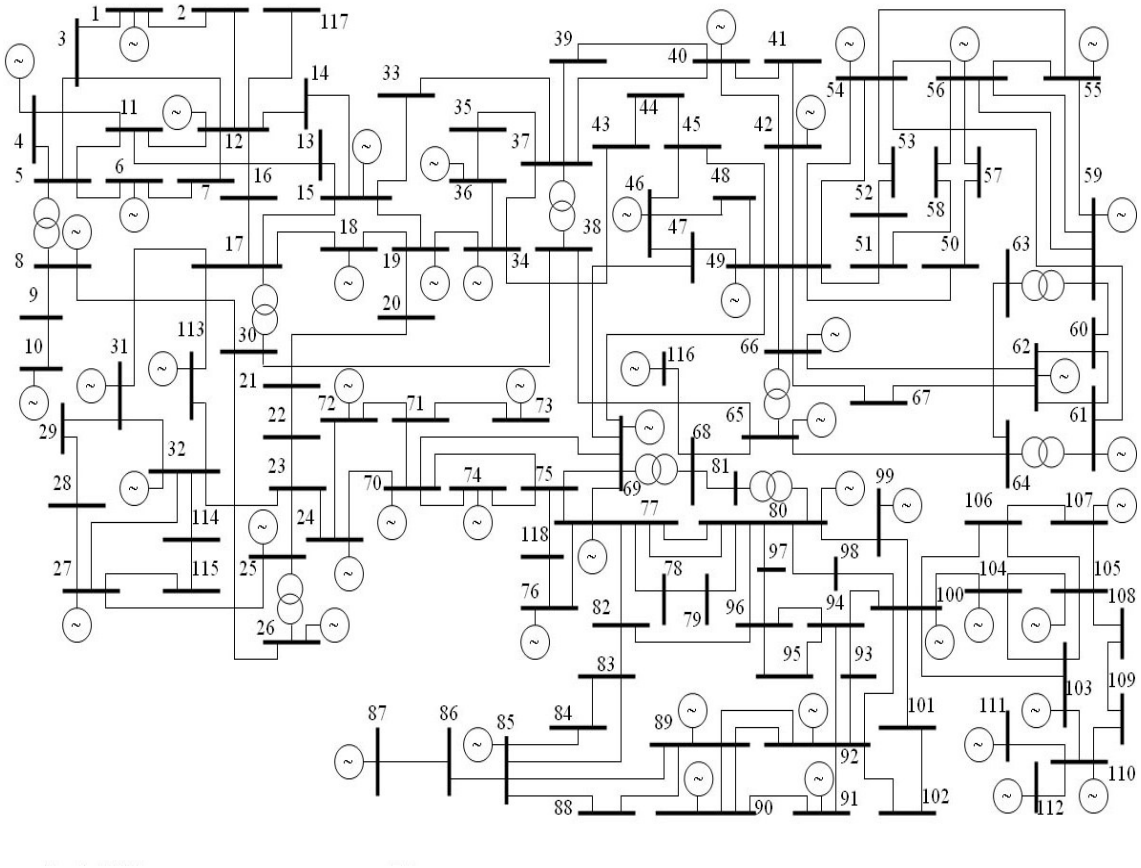

Figure 1: IEEE 118-Bus Test System

Table 1: IEEE 118-Bus Test System Case Summary

Case Information	
Name of Device	No. of Devices
Buses	118
Generators	54
Trans. Lines	177
Transformers	9
Loads	91
Islands	1
Slack Bus	1 (Bus 69)
Zones	1

Table 2: Case Totals

For In-service Devices		
	MW	Mvar
Load	4242.0	1438.0
Generation	4374.4	793.9
Shunts	0.0	-84.8
Losses	132.5	-559.7

Table 3: Generator General Information

Generator Information						
Generator Bus Number	Gen MW	Gen Mvar	Machine Model	Exciter	Stabilizer	Governor
10	450	-51.04	GENROU	IEEET1	IEEEST	IEEEG1
12	85	91.27	GENROU	IEEET1	IEEEST	IEEEG1
25	220	49.80	GENROU	IEEET1	IEEEST	IEEEG1
26	314	9.90	GENROU	IEEET1	IEEEST	IEEEG1
31	7	31.98	GENROU	IEEET1	IEEEST	IEEEG1
46	19	-5.23	GENROU	IEEET1	IEEEST	IEEEG1
49	204	115.65	GENROU	IEEET1	IEEEST	IEEEG1
54	48	3.90	GENROU	IEEET1	IEEEST	IEEEG1
59	155	76.83	GENROU	IEEET1	IEEEST	IEEEG1
61	160	-40.39	GENROU	IEEET1	IEEEST	IEEEG1
65	391	80.81	GENROU	IEEET1	IEEEST	IEEEG1
66	392	-1.95	GENROU	IEEET1	IEEEST	IEEEG1
69	513.39	-82.38	GENROU	IEEET1	IEEEST	IEEEG1
80	477	105.05	GENROU	IEEET1	IEEEST	IEEEG1
87	4	11.02	GENROU	IEEET1	IEEEST	IEEEG1
89	607	-11.79	GENROU	IEEET1	IEEEST	IEEEG1
100	252	110.06	GENROU	IEEET1	IEEEST	IEEEG1
103	40	40	GENROU	IEEET1	IEEEST	IEEEG1
111	36	-1.84	GENROU	IEEET1	IEEEST	IEEEG1

Table 4: Generator Modeling Parameter Data (Part 1)

Generator Information			
Machine Model parameter	PU value	Exciter parameter	PU value
H	3.00	T_r	0.00
D	0.00	K_a	50.00
R_a	0.00	T_a	0.80
X_d	2.10	Vr_{max}	1.00
X_q	0.50	Vr_{min}	-1.00
X_{dp}	0.20	K_e	-0.06
X_{qp}	0.50	T_e	0.06
X_{dpp}	0.18	K_f	0.09
X_l	0.15	T_f	1.46
T_{dop}	7.00	E_1	2.80
T_{qop}	0.75	SE_1	0.04
T_{dopp}	0.08	E_2	3.73
T_{qopp}	0.08	SE_2	0.33
S1	0.00		
R_{comp}	0.00		
X_{comp}	0.00		

Table 5: Generator Modeling Parameter Data (Part 2)

Generator Information			
Governor parameter	PU value	Stabilizer parameter	PU value
K	25.00	I_{cs}	1.00
T_1	0.00	A_1	1.013
T_2	0.00	A_2	0.013
T_3	0.10	A_3	0.00
U_o	1.00	A_4	0.00
U_c	-10.00	A_5	1.013
P_{max}	1.00	A_6	0.113
P_{min}	0.00	T_1	0.00
T_4	0.10	T_2	0.02
K_1	1.00	T_3	0.00
E_{ps}	0.00	T_4	0.00
Gv_1	0.00	T_5	1.65
P_{gv3}	0.00	T_6	1.65
		K_s	3.00
		Ls_{max}	0.10
		Ls_{min}	-0.10

Table 6: IEEE 118-Bus Test System Load Point Data

Load Information								
Load Bus Number	MW	Mvar	Load Bus Number	MW	Mvar	Load Bus Number	MW	Mvar
1	51	27	42	96	23	83	20	10
2	20	9	43	18	7	84	11	7
3	39	10	44	16	8	85	24	15
4	39	12	45	53	22	86	21	10
6	52	22	46	28	10	88	48	10
7	19	2	47	34	0	90	163	42
8	28	0	48	20	11	91	10	0
11	70	23	49	87	30	92	65	10
12	47	10	50	17	4	93	12	7
13	34	16	51	17	8	94	30	16
14	14	1	52	18	5	95	42	31
15	90	30	53	23	11	96	38	15
16	25	10	54	113	32	97	15	9
17	11	3	55	63	22	98	34	8
18	60	34	56	84	18	99	42	0
19	45	25	57	12	3	100	37	18
20	18	3	58	12	3	101	22	15
21	14	8	59	277	113	102	5	3
22	10	5	60	78	3	103	23	16
23	7	3	62	77	14	104	38	25
24	13	0	66	39	18	105	31	26
27	71	13	67	28	7	106	43	16
28	17	7	70	66	20	107	50	12
29	24	4	72	12	0	108	2	1
31	43	27	73	6	0	109	8	3
32	59	23	74	68	27	110	39	30
33	23	9	75	47	11	112	68	13
34	59	26	76	68	36	113	6	0
35	33	9	77	61	28	114	8	3
36	31	17	78	71	26	115	22	7
39	27	11	79	39	32	116	184	0
40	66	23	80	130	26	117	20	8
41	37	10	82	54	27	118	33	15

Appendix 2: Case Study II Data for the IEEE 39-Bus Test System

In case study II, the implementation of the ConvLSTM NN model is pursued on the IEEE 39-bus test system shown in Figure 2. The information regarding the case summary of the specified model is shown in Table 7 and 8. The transient stability analysis simulations are run in PowerWorld software environment for faults at each bus and transmission line. The machine model, exciter, governor and stabilizer of the generators and other general information are provided in Table 9. The values of the model parameters used for modeling the generator machines are shown in Table 10. The table includes generator information for 10 generators with real power data. Along with information regarding the power generation, the load point information at the base case is given in Table 11.

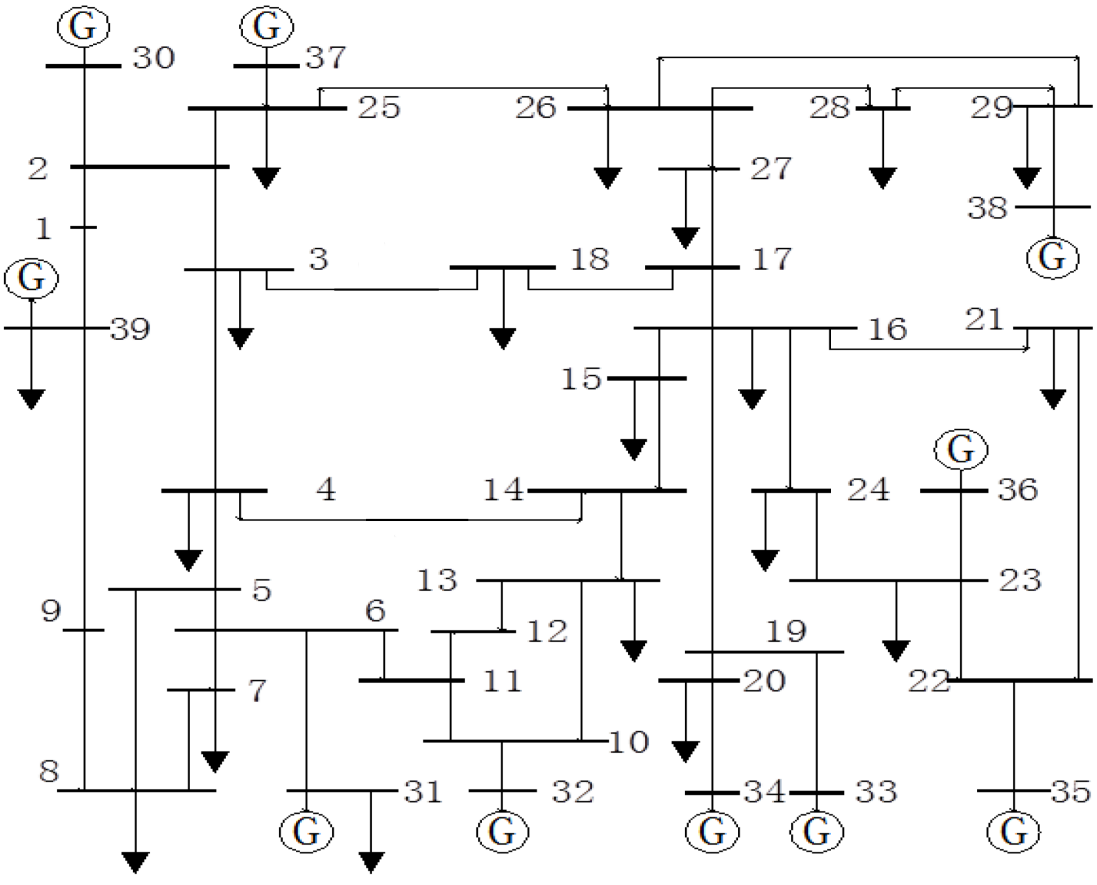

Figure 2: IEEE 39-Bus Test System

Table 7: IEEE 39-Bus Test System Case Summary

Case Information	
Name of Device	No. of Devices
Buses	39
Generators	10
Trans. Lines	34
Transformers	12
Loads	31
Islands	1
Slack Bus	1 (Bus 31)
Zones	1

Table 8: Case Totals

For In-service Devices		
	MW	Mvar
Load	6149.5	1408.9
Generation	6191.3	837.3
Shunts	0.0	-342.7
Losses	41.8	-228.9

Table 9: Generator General Information

Generator Information					
Generator Bus Number	Gen MW	Gen Mvar	Machine Model	Exciter	Stabilizer
30	250	83.21	GENCLS	ESDC1A	STAB1
31	571.28	363.94	GENCLS	ESDC1A	STAB1
32	650	1.53	GENCLS	ESDC1A	STAB1
33	632	69.67	GENCLS	ESDC1A	STAB1
34	508	148.79	GENCLS	ESDC1A	STAB1
35	650	167.04	GENCLS	ESDC1A	STAB1
36	560	75.45	GENCLS	ESDC1A	STAB1
37	540	-35.35	GENCLS	ESDC1A	STAB1
38	830	-0.47	GENCLS	ESDC1A	STAB1
39	1000	-36.49	GENCLS	ESDC1A	STAB1

Table 10: Generator Modeling Parameter Data

Generator Information					
Machine Model parameter	PU value	Exciter parameter	PU value	Stabilizer	PU value
H	34.80	T_r	0.00	K_T	0.1061
D	0.00	K_a	5.00	T	10.00
R_a	0.00	T_a	0.02	T_1_T_3	0.50
X_{dp}	0.05	T_b	0.00	T_3	0.10
R_{comp}	0.00	T_c	0.00	T_2_T_4	0.50
X_{comp}	0.00	Vr_{max}	5.00	T_4	0.05
		Vr_{min}	-5.00	H_{lim}	0.20
		K_e	1.00		
		T_e	0.471		
		K_f	0.08		
		T_{f1}	1.25		
		E_1	3.00		
		SE_1	0.08		
		E_2	4.00		
		SE_2	0.25		
		UEL	0.00		
		exclim	0.00		

Table 11: IEEE 39-Bus Test System Load Point Data

Load Information		
Load Bus Number	MW	Mvar
1	0.00	0.00
2	0.00	0.00
3	333.00	2.40
4	500.00	184.00
5	0.00	0.00
6	0.00	0.00
7	233.80	84.00
8	522.00	176.00
9	0.00	0.00
10	0.00	0.00
11	0.00	0.00
12	7.50	88.00
13	0.00	0.00
14	0.00	0.00
15	320.00	153.00
16	329.40	32.30
17	0.00	0.00
18	158.00	30.00
19	0.00	0.00
20	680.00	103.00
21	274.00	115.00
22	0.00	0.00
23	247.50	84.60
24	308.60	-92.20
25	224.00	47.20
26	139.00	17.00
27	281.00	75.50
28	206.00	27.60
29	283.50	26.90
31	9.20	4.60
39	1104.00	250.00